Background

Heavy timber is a renewable natural resource:

- Offers a green alternative to conventional construction materials for buildings considering life cycle performance
- Light weight

- Heavy timber gravity resisting system with concrete core SFRS (Smith, 2016)
- 18 storey, world's tallest timber structure

UBC Brock Commons (2017)

27

Heavy Timber-Steel Structural System

- Heavy timber braced frame with capacity protected connections

- Glued-laminated timber columns and beams
- Cross-laminated timber (CLT) floor panels
- Glued-in rod connections (Gilbert and Erochko 2016)

- BRB

Self-centering telescoping braces
Friction damper braces

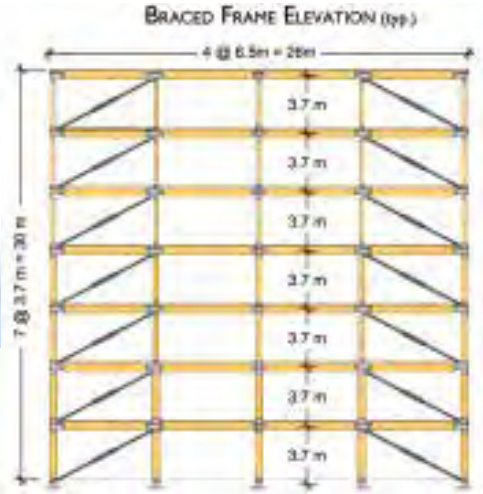

28

Glued-in-rod Connection

Efficient connection
Transfers force parallel to grain
Ease of construction

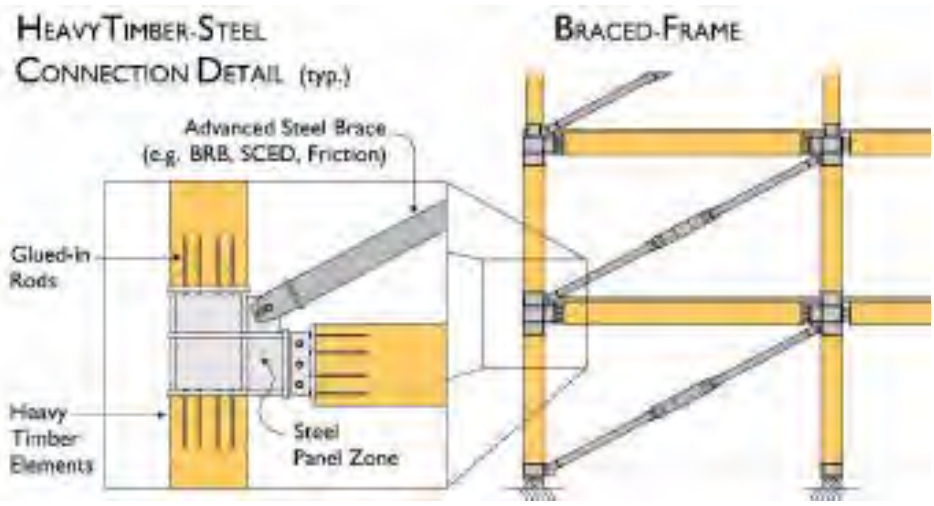

Friction Braces

- High energy dissipation (large flag shape hysteresis)
- Brass-Stainless Steel friction interface
- Similar dynamic and static friction coefficients

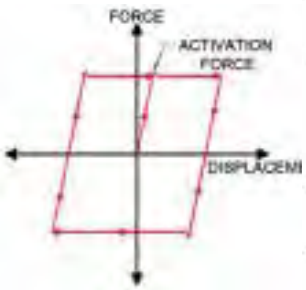

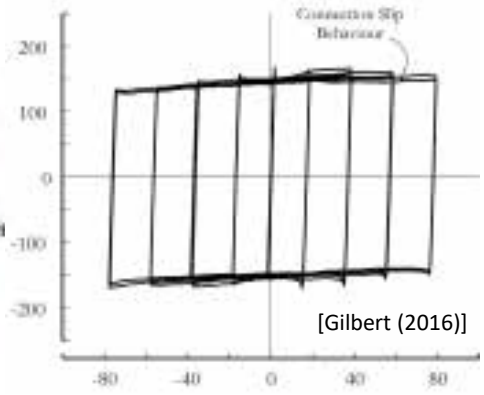

[Gilbert (2016)]

30

Hybrid Simulation Numerical Substructure

- OpenSees (McKenna et al., 2000)

PLan

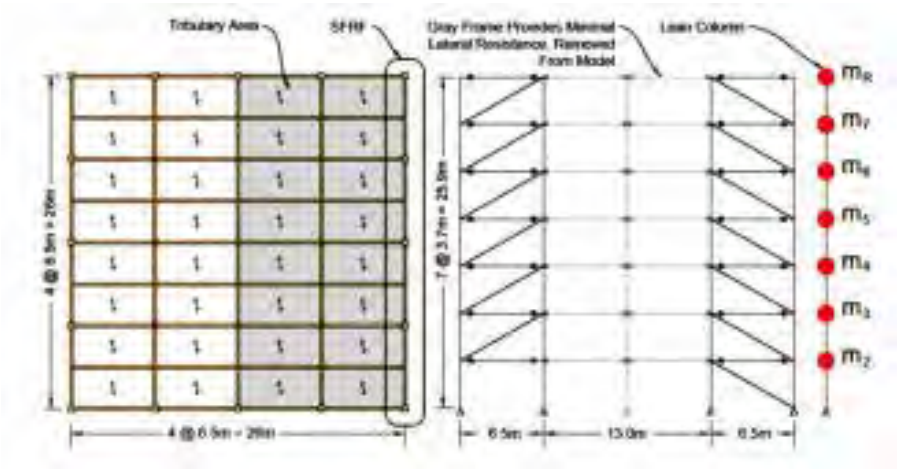

Elevation

31

Substructuring Approach

Experimental Substructure

Analytical Substructure

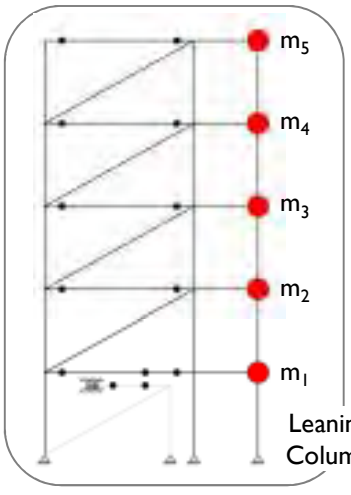

- Mass in analytical model;
- Single bay of the multi-bay structure modelled
- First story experimental substructure
- Elements modelled using 2D beam-column elements.

OpenSees

OpenFresco

Middleware

Substructuring Approach

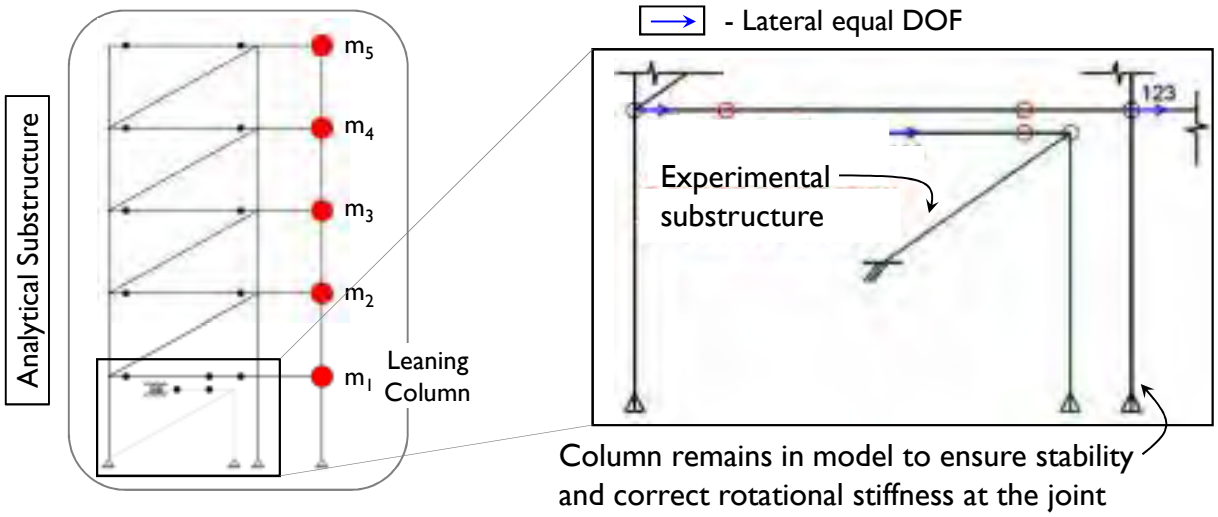

Experimental Test Setup

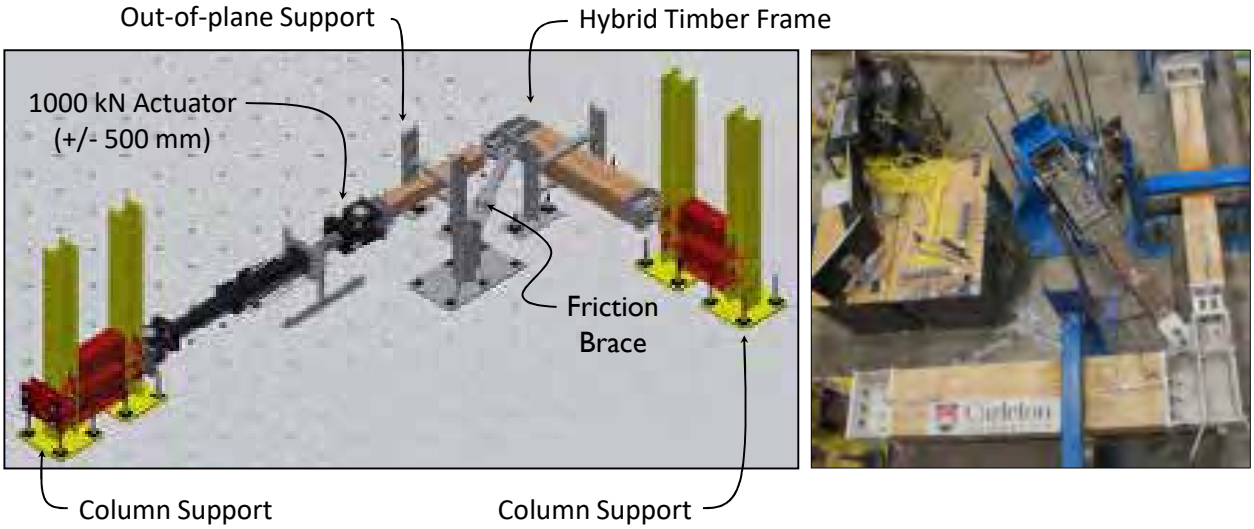

Hybrid Simulation Results

Heavy Timber Frame Hybrid Simulation
1987 Imperial Valley Eq. Record (320%)

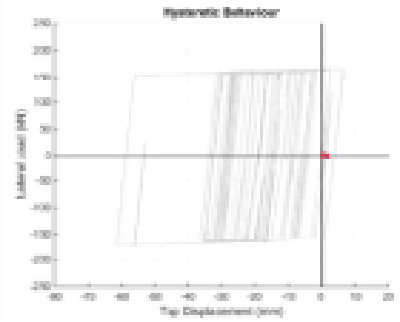

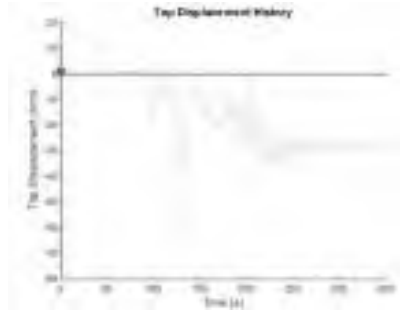

Hybrid Simulation Results

- Hybrid simulation results show good agreement with FE models;
- Differences attributed to zero post-yield stiffness friction brace.

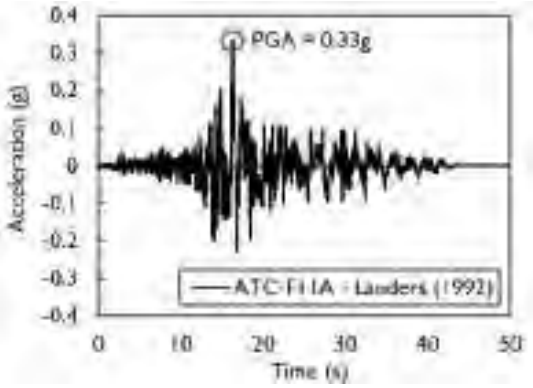

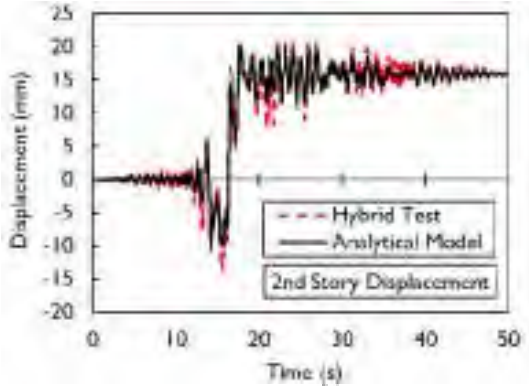

Incremental Dynamic Simulation

- Assessment of the heavy timber-steel structural system behaviour under increasing seismic hazard intensity
- Analytical and Experimental (hybrid) IDA
  - 11 far field earthquake records
  - Scaled as a suite
  - Generate maximum inter-storey drift IDA curves
  - Generate maximum residual inter-storey drift IDA curves

37

Incremental Dynamic Analysis (IDA)

- IDA used to further study the seismic behaviour of the prototype structure over the full range of its dynamic response

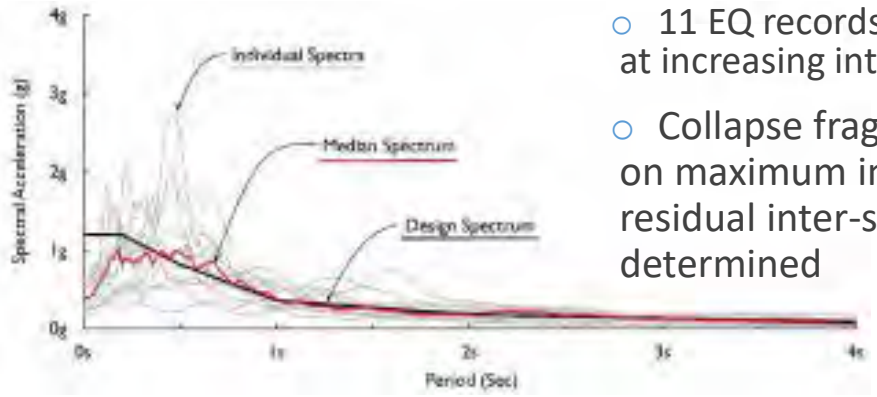

- 11 EQ records (ATC 2009) applied at increasing intensities to collapse
- Collapse fragility curves based on maximum inter-story drift and residual inter-story drift are determined

Incremental Dynamic Analysis Results

Maximum Inter-Story Drift

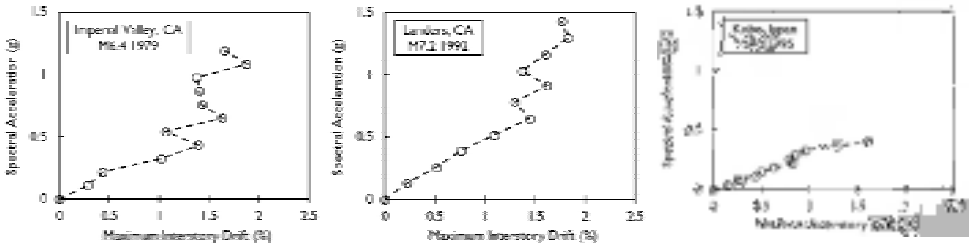

Maximum Inter-Story Residual Drift

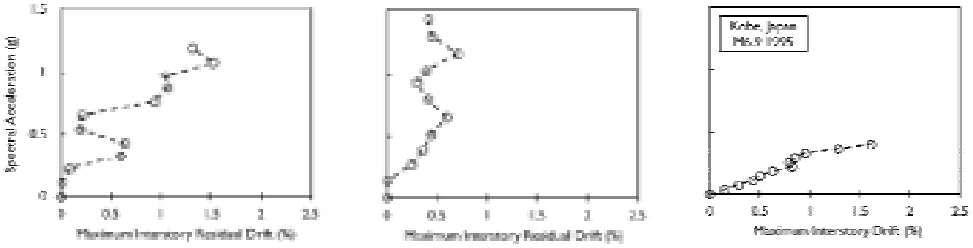

- Results show weaving, hardening, and softening behavior under different EQs

Maximum Inter-storey Drift

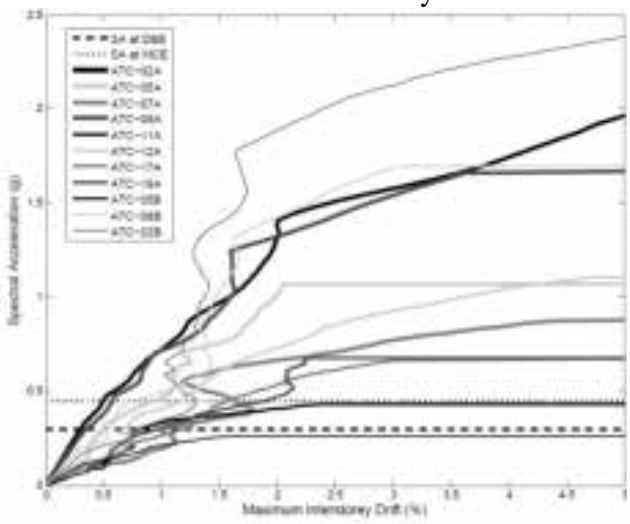

Maximum Residual Inter-storey Drift

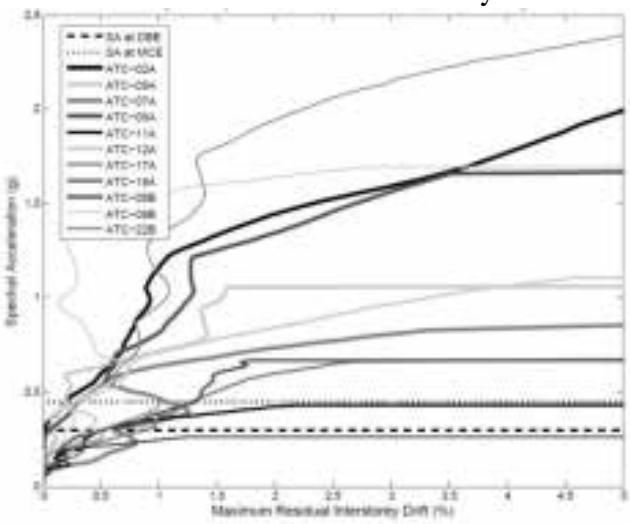

40

Fragility Curves

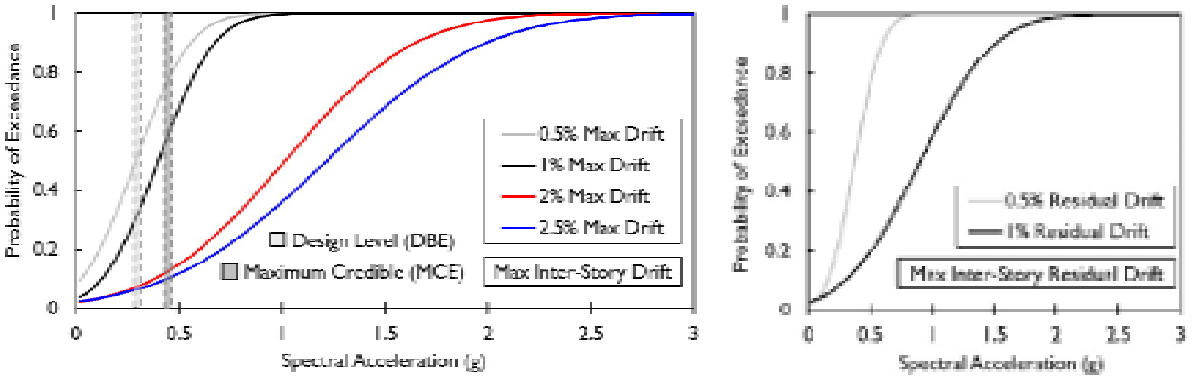

- Probability of reaching life-safety performance limit < 15% at MCE;
- Probability of exceeding 0.5% residual drift is 65% at MCE.

Earthquake Response and Repair of a Multi-Storey RC Shear Wall using Hybrid Simulation

Josh Woods, Postdoctoral Fellow, Ecole Polytechnique Montreal
David Lau, Jeffrey Erochko, Carleton University, Ottawa

Carleton UNIVERSITY

Past Studies

Hybrid Simulation of a RC Shear Wall (Whyte and Stojadinovic, 2013)

- Large-scale single storey RC squat shear wall, representative of nuclear facility;
- Treated as a SDOF system;
- Mass modelled using OpenSees;

Objectives

- Investigate the feasibility of using a displacement-based hybrid simulation formulation to study the seismic response of a multi-storey RC structure;
- Develop a detailed finite element model of the analytical substructuring using layered shell elements in OpenSees to predict wall earthquake response;
- Study the challenges associated with hybrid simulation of a stiff RC structure;

Prototype Shear Wall Structure

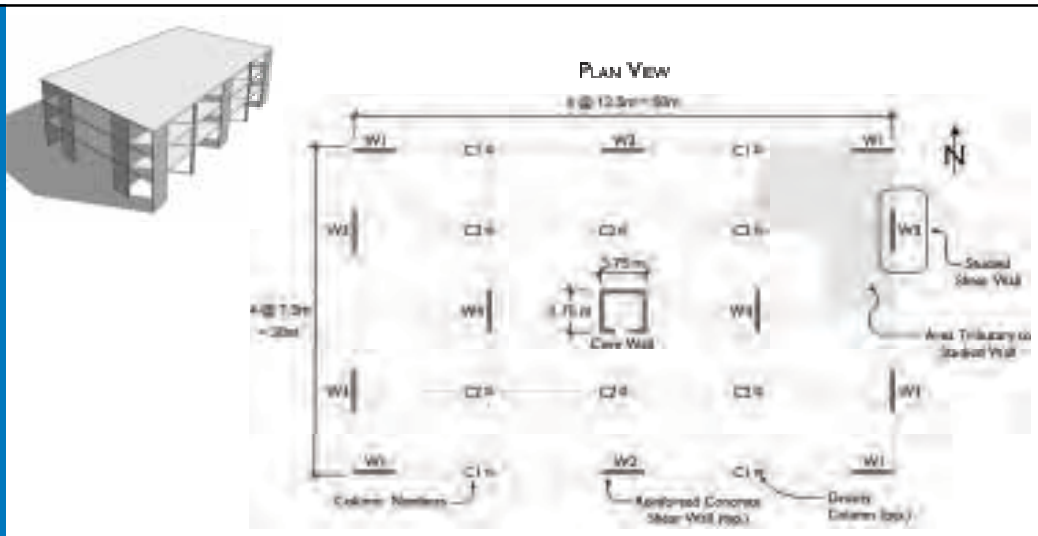

- 3-Storey Shear Wall Building
- Located in Victoria, British Columbia
- Gravity Load Resisting System: Flat Plate Slab and Columns
- Lateral Load Resisting System: Moderately Ductile Shear Walls

Prototype Shear Wall Structure

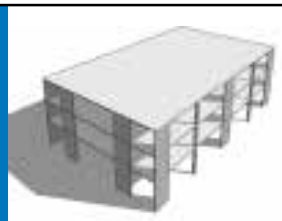

- Equivalent Static Force Procedure (NBCC, 2015)
- Response Spectrum Analysis (High Seismicity: $I_E F_a S_a(0.2) > 0.35$)
- Fundamental Period within NBCC, 2015 limits ($T_a \leq T \leq 2T_a$)
- Torsional Sensitivity ($B_x/B_y < 1.7$)

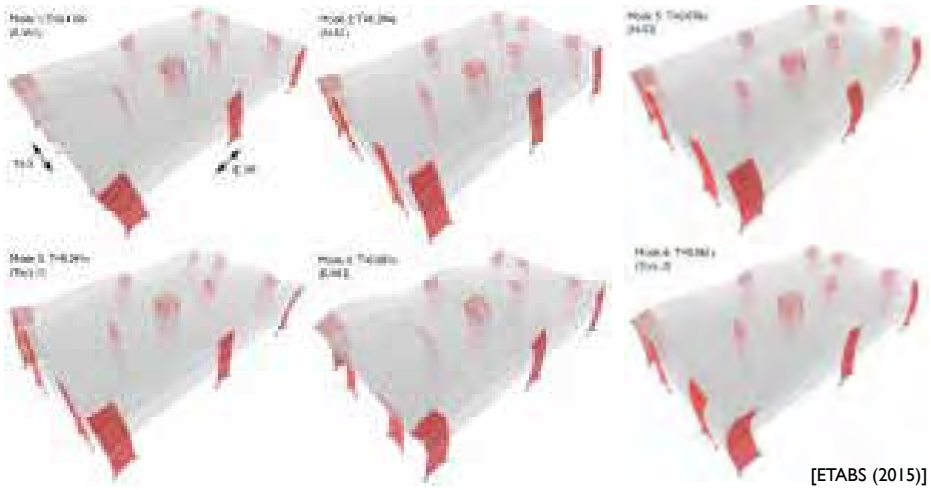

[ETABS (2015)]

Prototype Shear Wall Structure

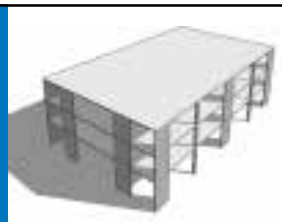

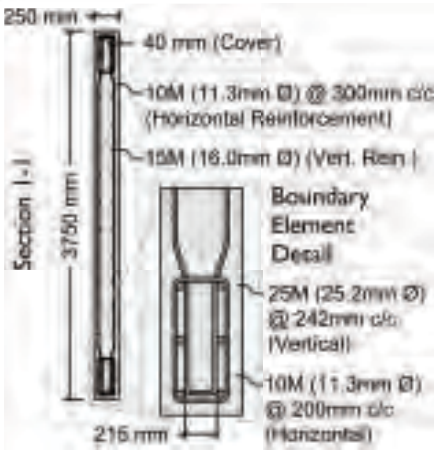

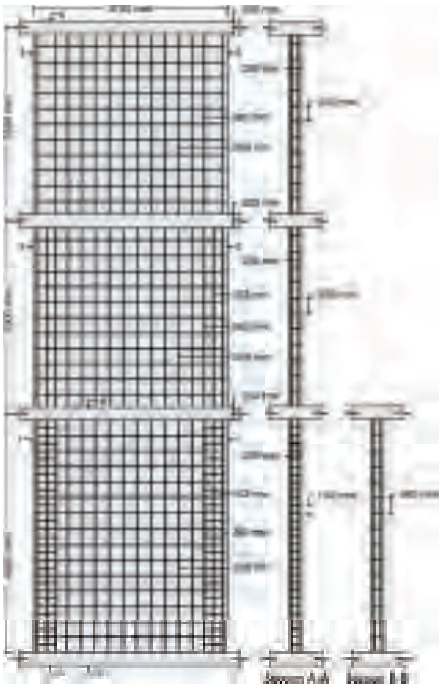

Analytical & Experimental Substructures

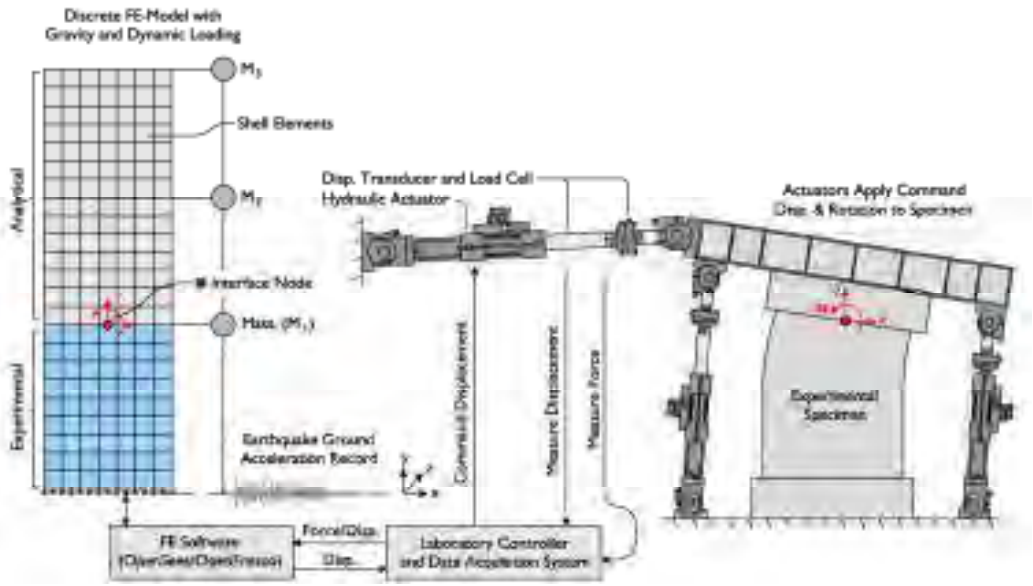

OpenSees [McKenna et al. (2000)]

OpenFres [Schellenberg et al. (2009)]

MTS Flextest Controller

Analytical Substructure

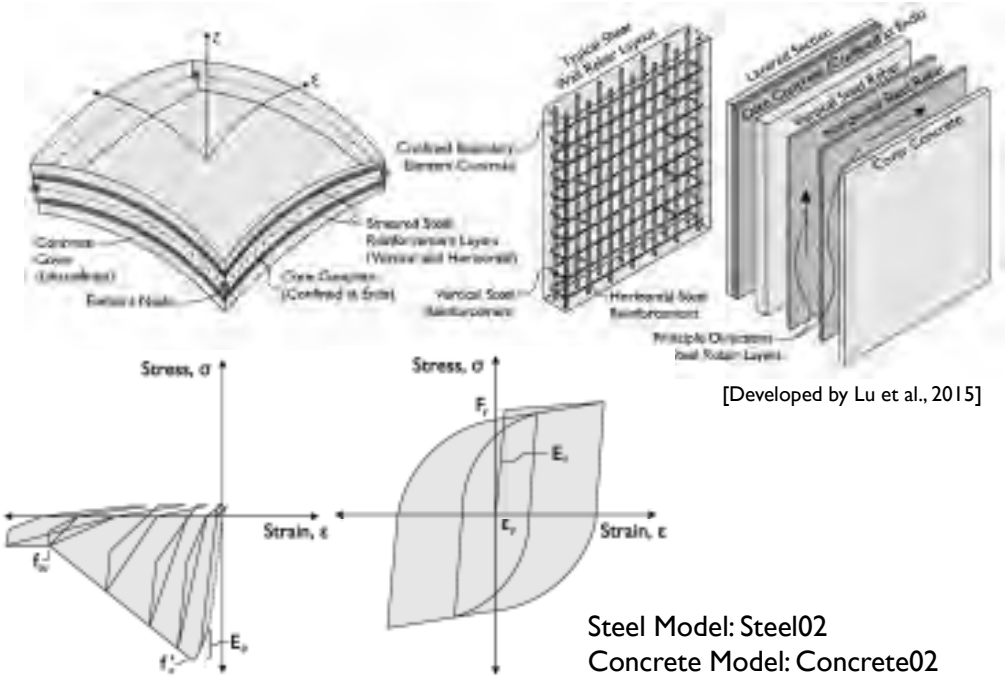

[Developed by Lu et al., 2015]

Steel Model: Steel02
Concrete Model: Concrete02

Experimental Substructure

- Experimental substructure scaled to 40% of its original size to accommodate for space limitations in the laboratory

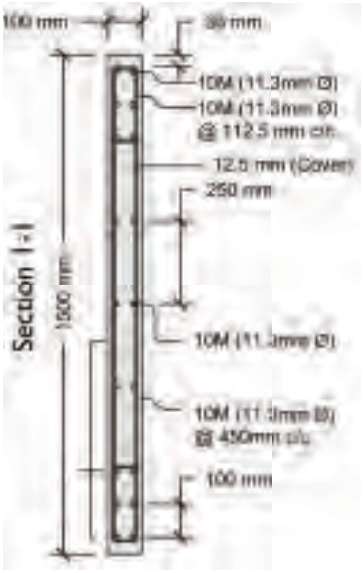

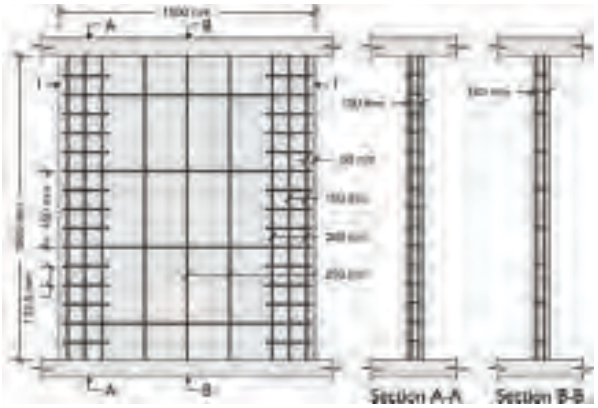

Matches wall dimensions tested under static cyclic load:

- Lombard et al. (2000)
- Hiotakis (2004)
- Woods et al. (2016)

Experimental Test Setup

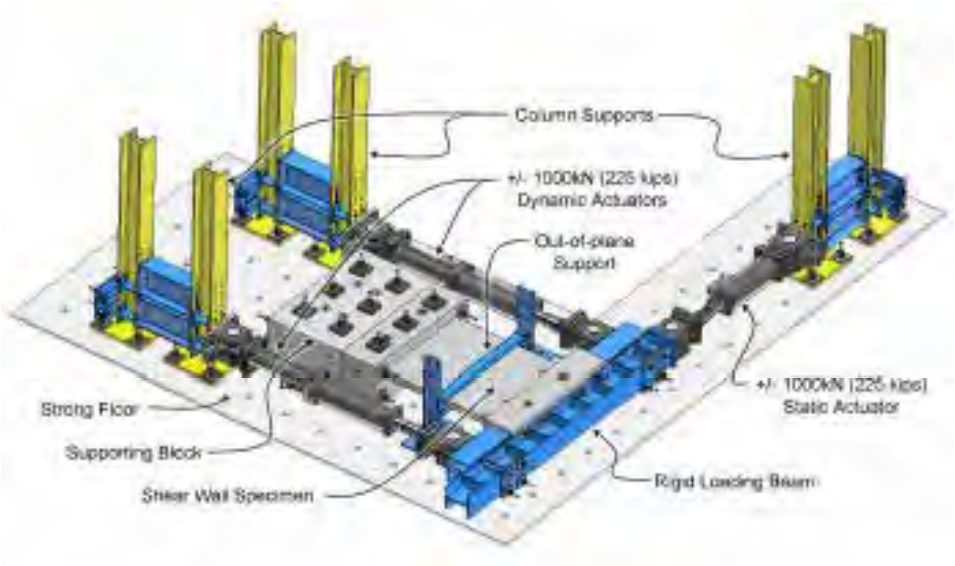

Experimental Substructure

Experimental Test Setup

Challenges for Stiff Structures

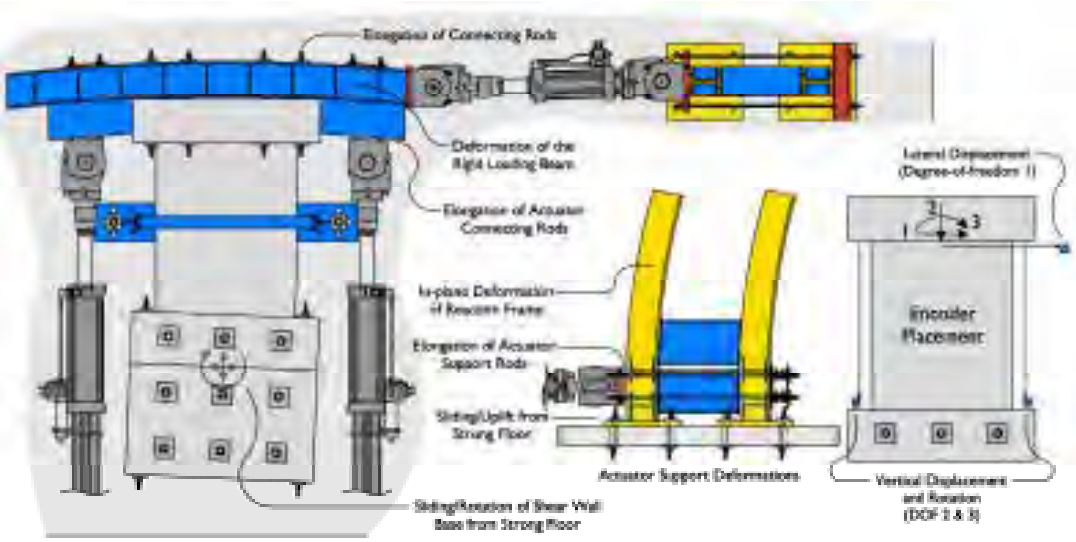

- Small command displacement results in a large jump in force;
- Deformation of the test setup could impact quality of results;

High-precision Encoders for External Control

- High precision (0.028mm measurement resolution) encoders;
- Used to externally control the hybrid simulation;
- Measure/feedback the vertical and lateral displacements and rotation;
- Use of the encoders bypasses deformation of the setup for more accurate hybrid simulation results;

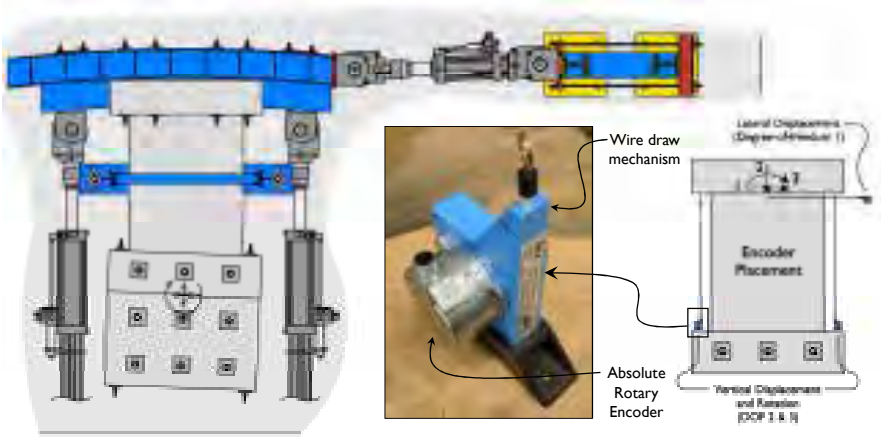

Challenges for Stiff Structures

- Implement simultaneous geometric transformations for force/moment and displacement/rotation using the MTS DOF Control software
- Ideal for multi-actuator setups and over-constrained systems

Displacement/Rotation Transformation ✚ Force/Moment Transformation

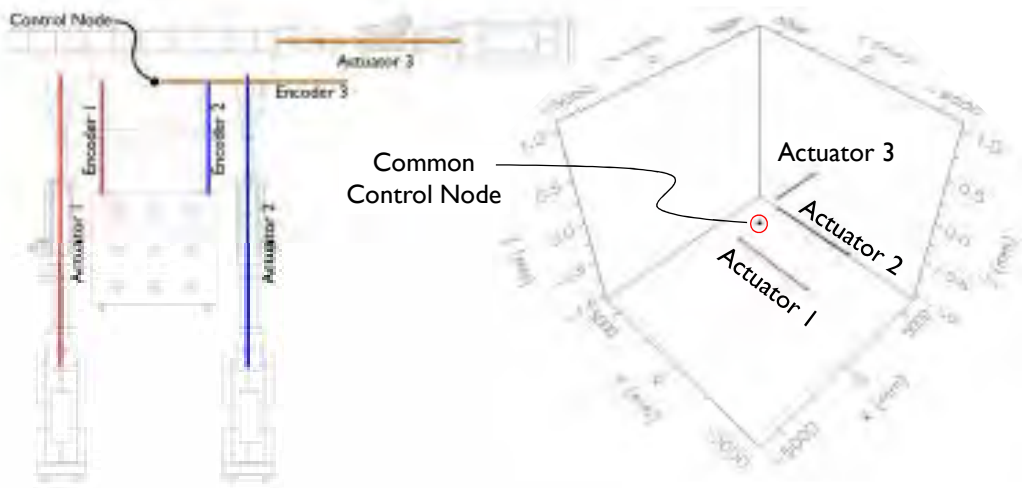

Challenges for Stiff Structures

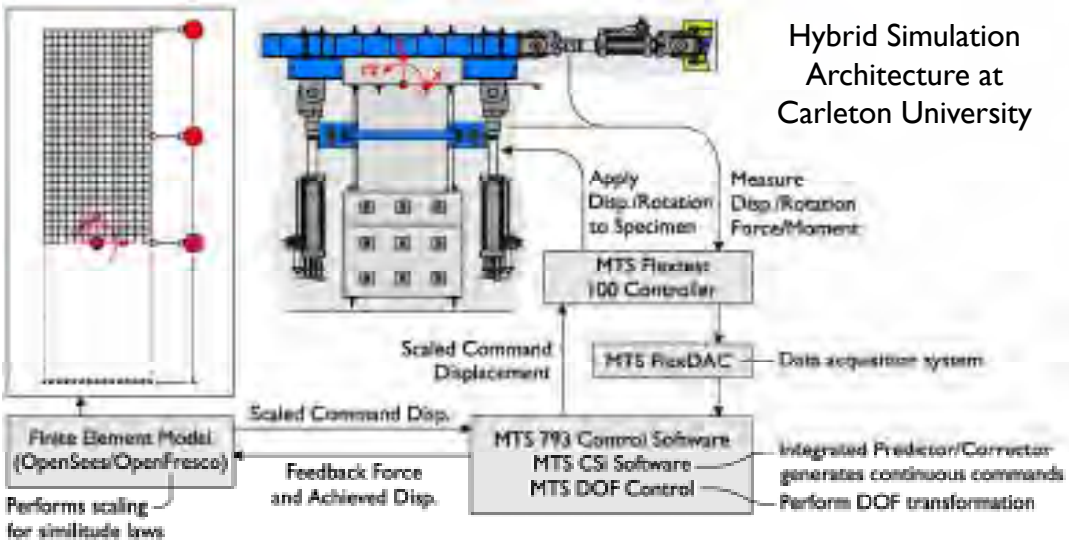

Challenges for Stiff Structures

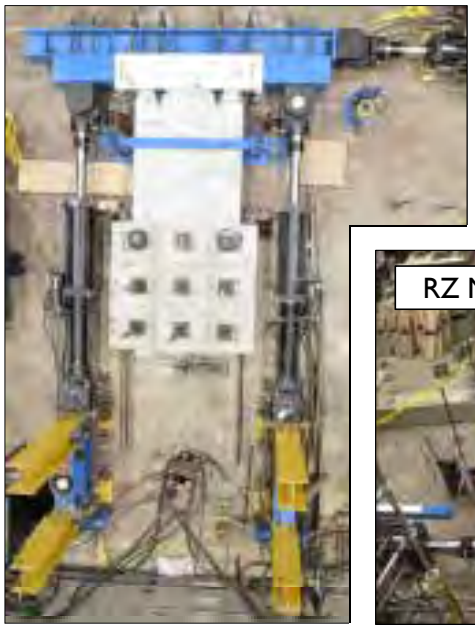

- Experiment controlled based on X/Y displacement and Z rotation at control node;
- Hybrid simulation controlled externally using high-precision encoders;
- Safety limits based on actuator displacements and load cells;

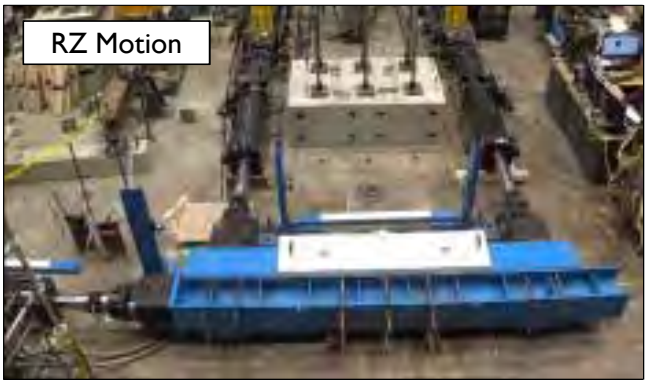

Hybrid Testing Control Station

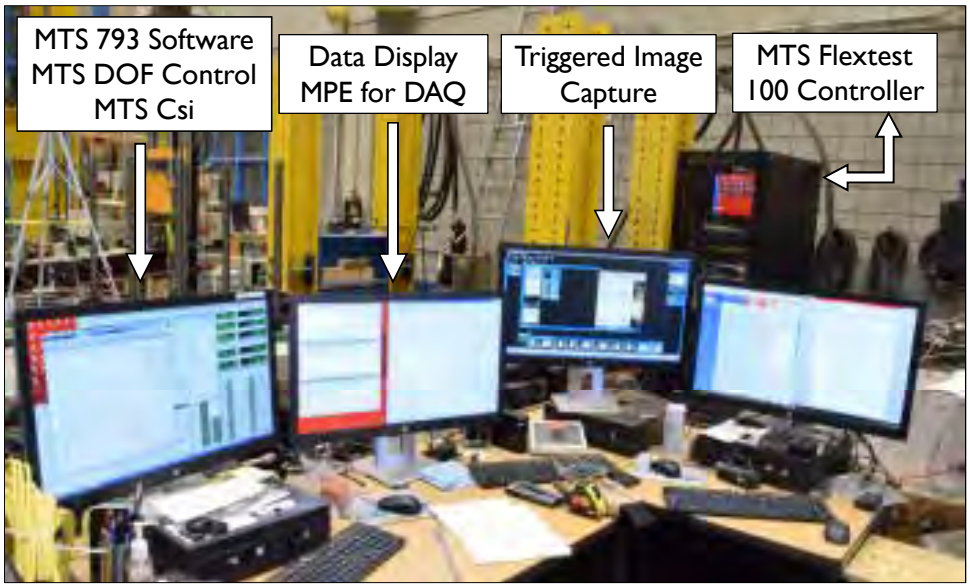

Instruments

LVDT Positions

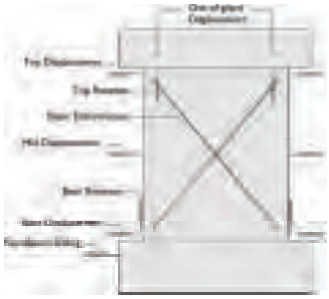

Strain Gauge Locations

Vertical Steel Rebar

Horizontal Steel Rebar

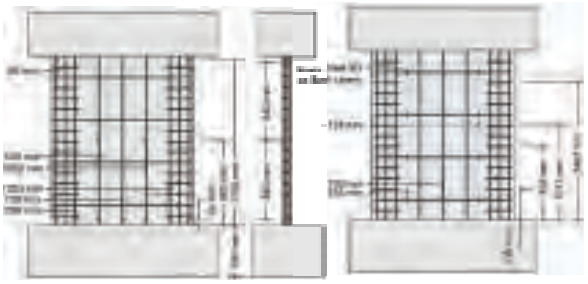

Digital Image Correlation

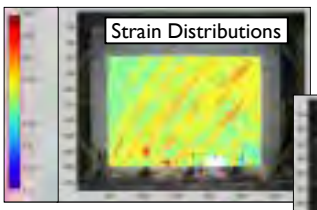

Developed by Dr. Yuan-Sen Yang
National Taipei University of
Technology (NTUT)

[Woods et al. (2016)]

Image Analysis

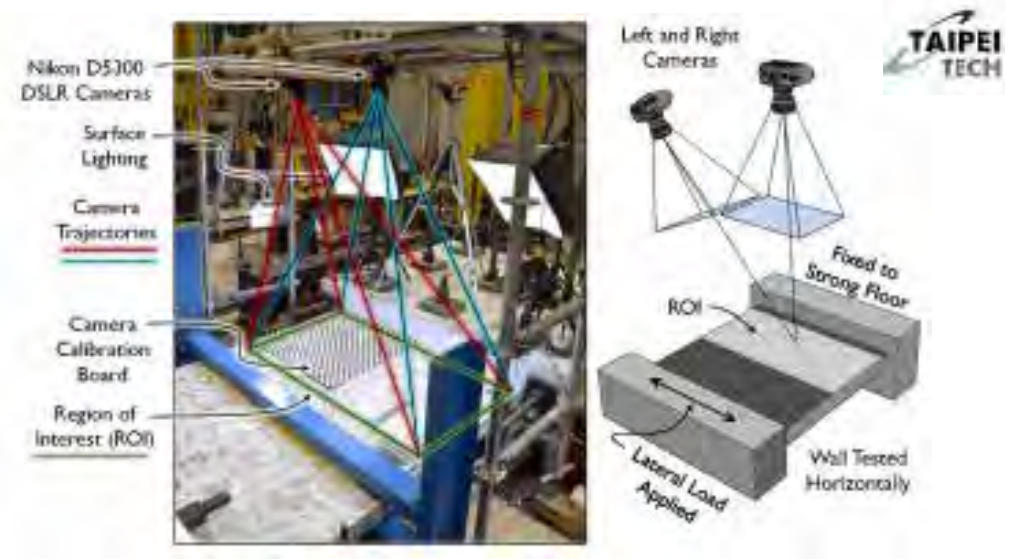

- Freely-available image analysis tool to measure displacement, crack, and strain fields;
- Developed at National Taipei Institute of Technology by Professor Yang;
- Avoids having to stop the test to mark cracks or approach a loaded specimen;

Earthquake Sequence

1994 Northridge Earthquake
Canoga Station Park Record
Magnitude: 6.7
Duration: 25 seconds
Applied in increasing intensity;

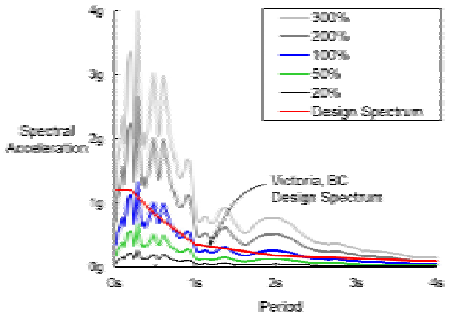

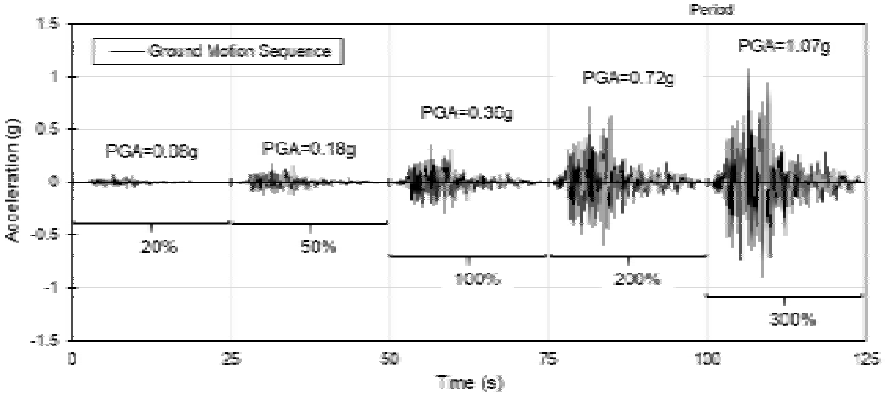

Test Results

Northridge Earthquake 200%

Input Ground Motion

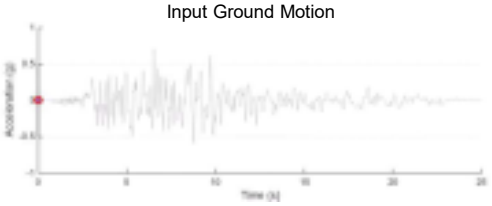

X Displacement Time History

Z Rotation Time History

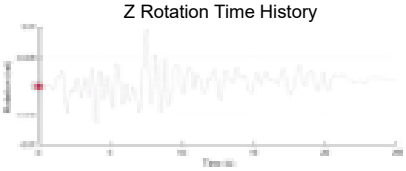

Force Displacement Hysteresis

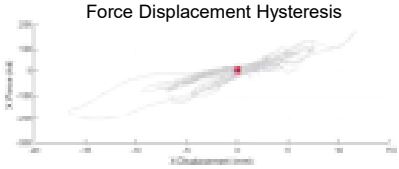

Moment Rotation Hysteresis

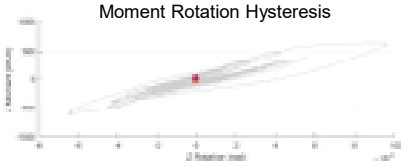

Test Results

Northridge Earthquake 200%

- Effectively tracks formation and propagation of concrete cracks

Control Wall Damage

Concrete Crushing at Base

Extensive Concrete Cracking

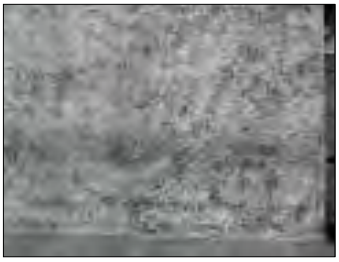

Comparison with Analytical Modelling Results

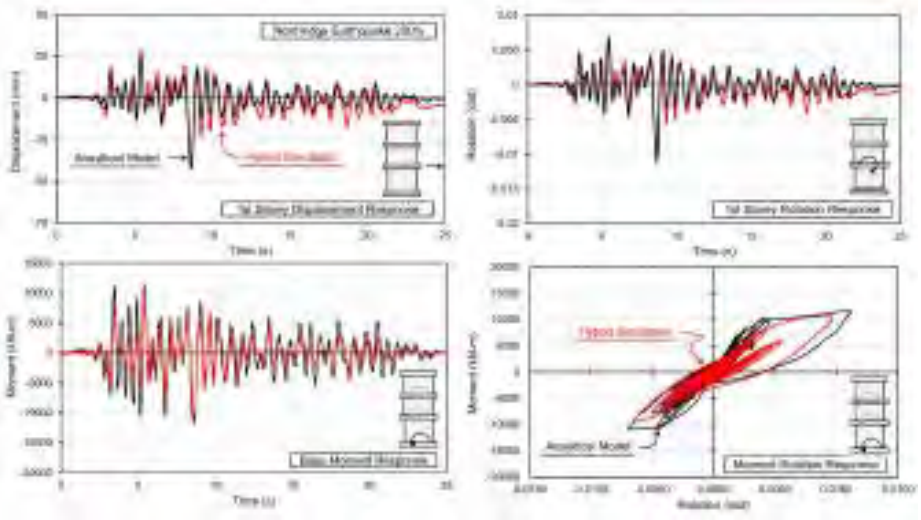

- Fully analytical model captures strength, stiffness, and nonlinear hysteretic response of the multi-storey shear wall;

Rehabilitation of Control Using CFRP Sheets

Epoxy Crack Injection | Shear Wall Front | Shear Wall Back

- Attempt to make CFRP repair more efficient by applying CFRP sheets to only one side of the concrete shear wall
- Reduce the operational downtime of a structure following an earthquake

Rehabilitation of Control Using CFRP Sheets

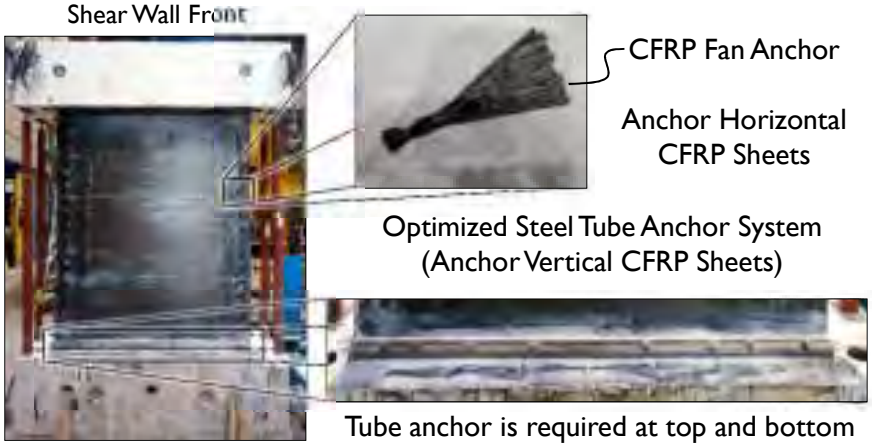

- Combination of mechanical and FRP anchorage to prevent debonding
- Further optimization of the tube anchor to improve constructability

Steel Tube Anchor System

- Based on pulley principle
- Transfers force carried by CFRP sheet without eccentricity
- Larger utilization of high strength capacity of CFRP sheets

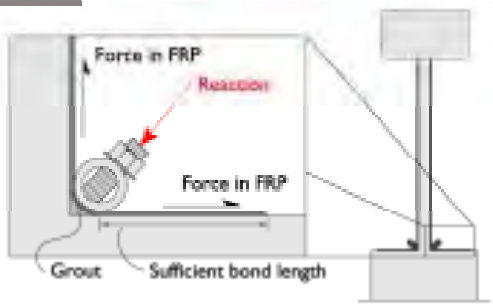

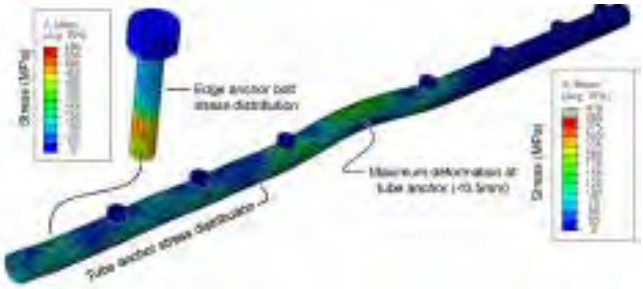

- Finite element modelling used to optimize tube anchor efficiency

*Tube anchor system: US Patent No. US20050252142; Canadian Patent No. CA2463363

Retrofit Results

- Initial stiffness response:

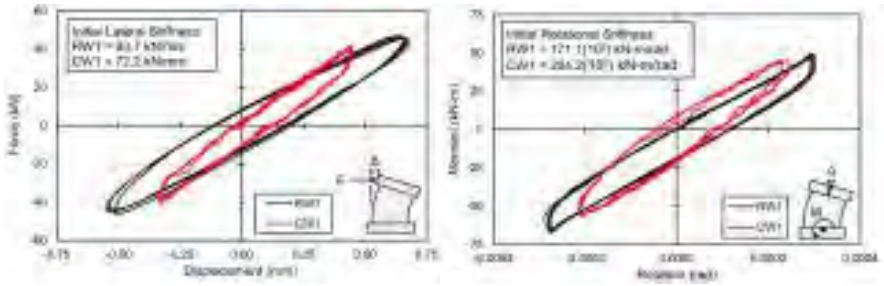

- Response comparison under design-level earthquake (DBE):

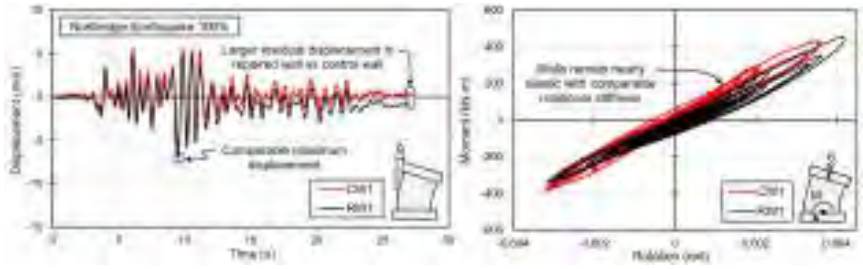

Northridge Earthquake – Canoga Park Station (200%)

Displacement-Time History

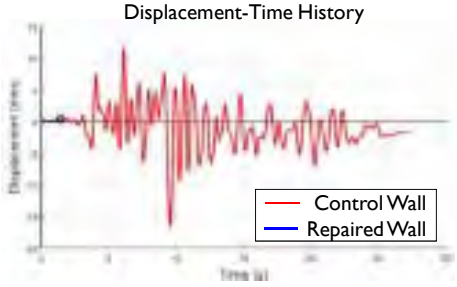

Moment-Rotation Hysteresis

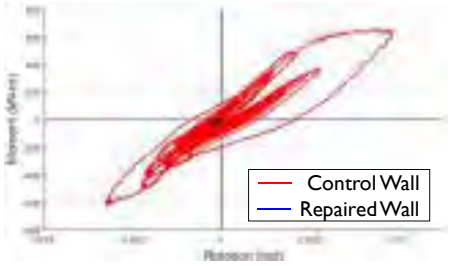

Woods, J., Erochko, J., and Lau, D.T. (2019). Hybrid Simulation of a Multi Story RC Shear Wall Retrofitted with Externally Bonded CFRP Sheets. *Journal of Composites for Construction.* (In-progress)

Retrofit Results

- Aftershock event (Northridge 150%):

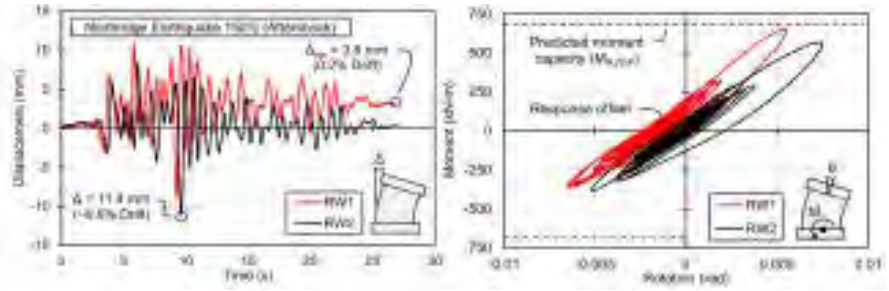

- Residual strength measured using cyclic testing with axial load:

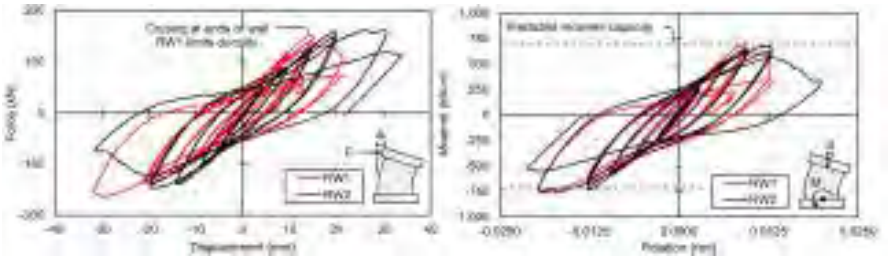

Damage to Repaired Wall

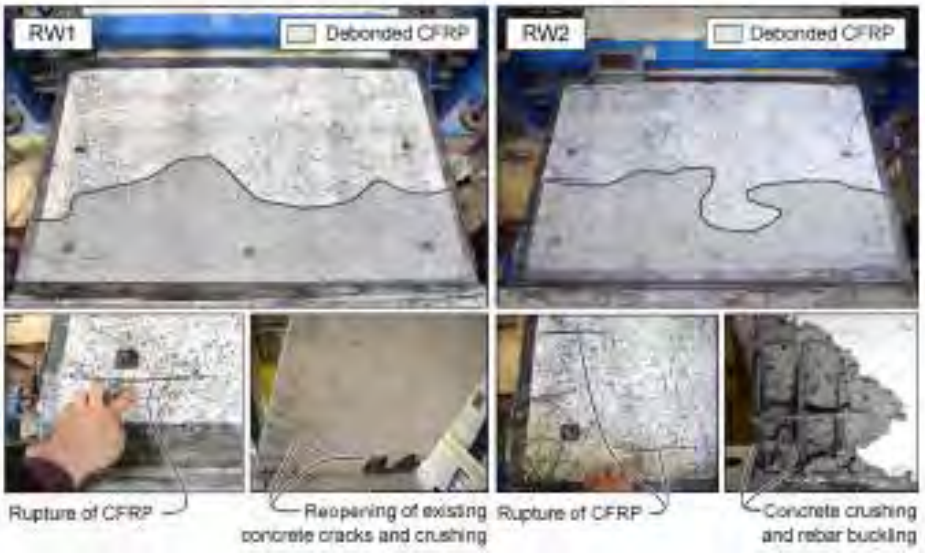

- Tube anchor allows CFRP sheet to rupture in tension in both walls

Conclusions

- Hybrid simulation provides an efficient method for capturing the overall system-level seismic performance of a structure;
- A three-storey prototype RC shear wall building has been designed in Victoria, BC and is the subject of the hybrid simulation;
- Hybrid simulation shown to be a useful tool to study the earthquake response of a multi-story RC shear wall and assess the performance of the CFRP retrofit under real earthquake ground motion records;
- The application of the CFRP retrofit completely restores the strength and the stiffness of the original wall (operational and design levels);
- Tube anchor system shown to performance well in transferring the force carried by the CFRP sheets and ruptures in tension.

IMPROVING THE SEISMIC PERFORMANCE OF EXISTING BRIDGE STRUCTURES USING SELF-CENTERING DAMPERS

Xi Cheng, JDavid Lau, effrey Erochko

Ottawa-Carleton Bridge Research Institute
Carleton University, Ottawa, Canada

Carleton UNIVERSITY

Self-Centering Energy Dissipative (SCED) Braces

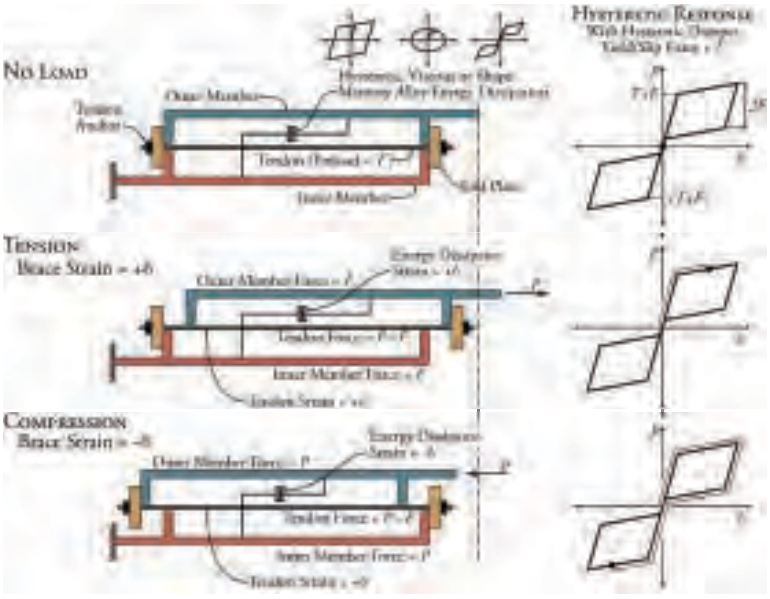

Note : Figures from (Erochko 2014)

Self-Centering Energy Dissipative (SCED) Braces

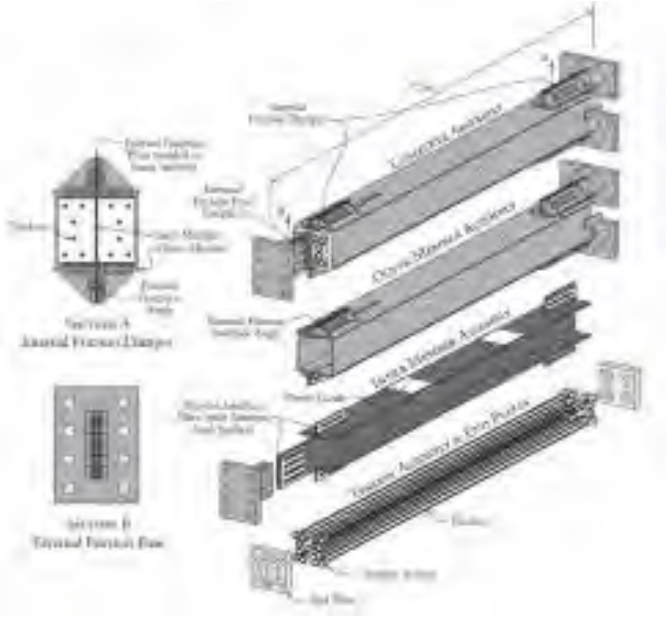

Self-Centering Energy Dissipative (SCED) Braces

Static Cyclic Tests

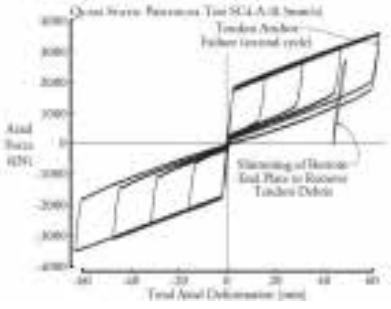

Dynamic Tests

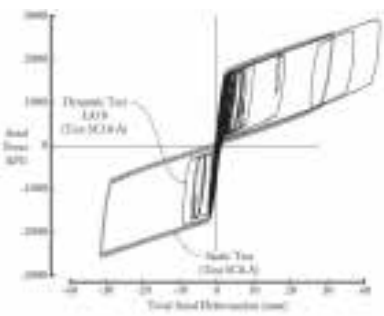

J Erochko, U Toronto

Example Bridge: Two-Span Bridge (M1)

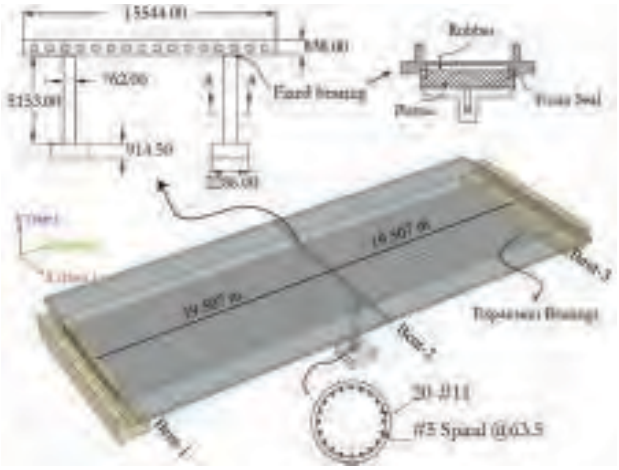

Geometry of Two-Span Bridge (M1)

Seismic Zones (NBCC 1970)

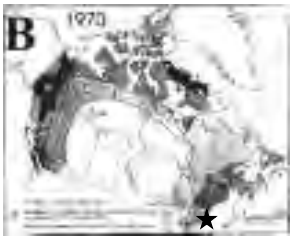

(J. Adams 2012)

Simplified Seismic Hazard Map (NBCC 2015)

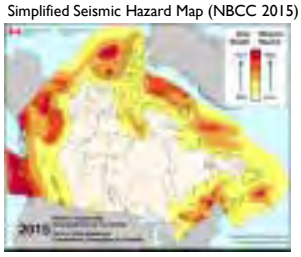

Self-Centering Brace Retrofit Bridges

X. Cheng, J. Erochko, D. Lau

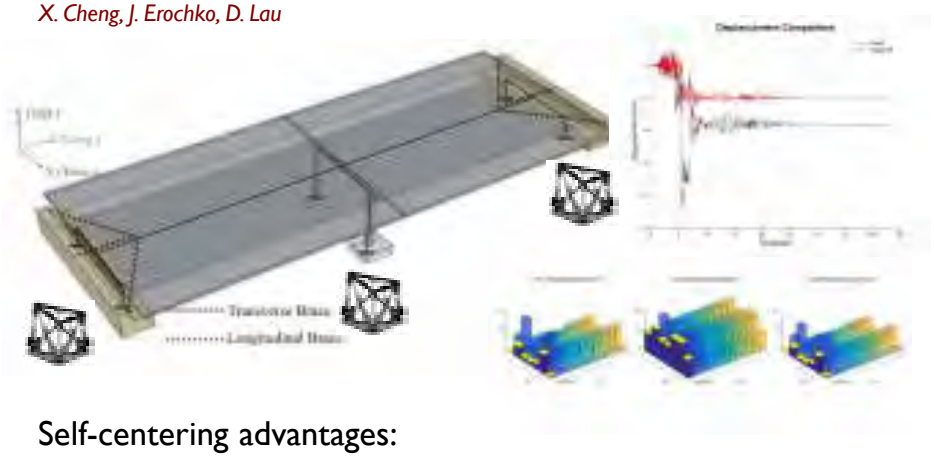

Self-centering advantages:

- Even with less energy dissipation, but restore the structure to (or close to) original position
- Reduce cumulative damage to the structure

Performance: Displacement Time History Example

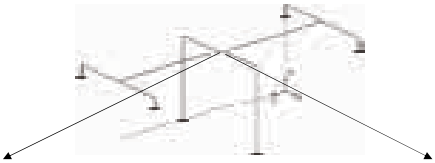

Transverse Displacement

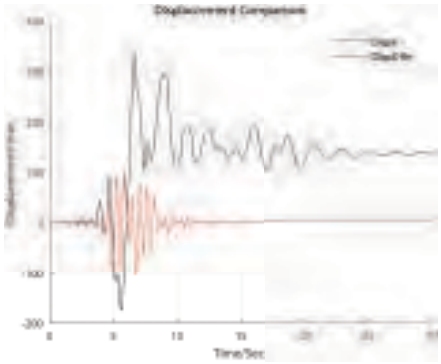

Longitudinal Displacement

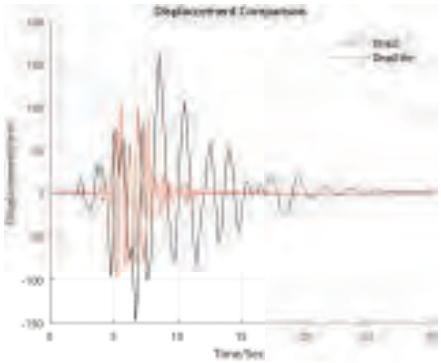

Earthquake-Fire Coupled Hybrid Simulation

David Lau [1], Jeffrey Erochko [1], Zhimeng Yu [1], Ahmed Kashef [2], Oh-Sung Kwon [3]

[1] Ottawa-Carleton Multi-Hazard Research Centre, Carleton University

[2] NRC Fire Laboratory, National Research Council of Canada

[3] University of Toronto

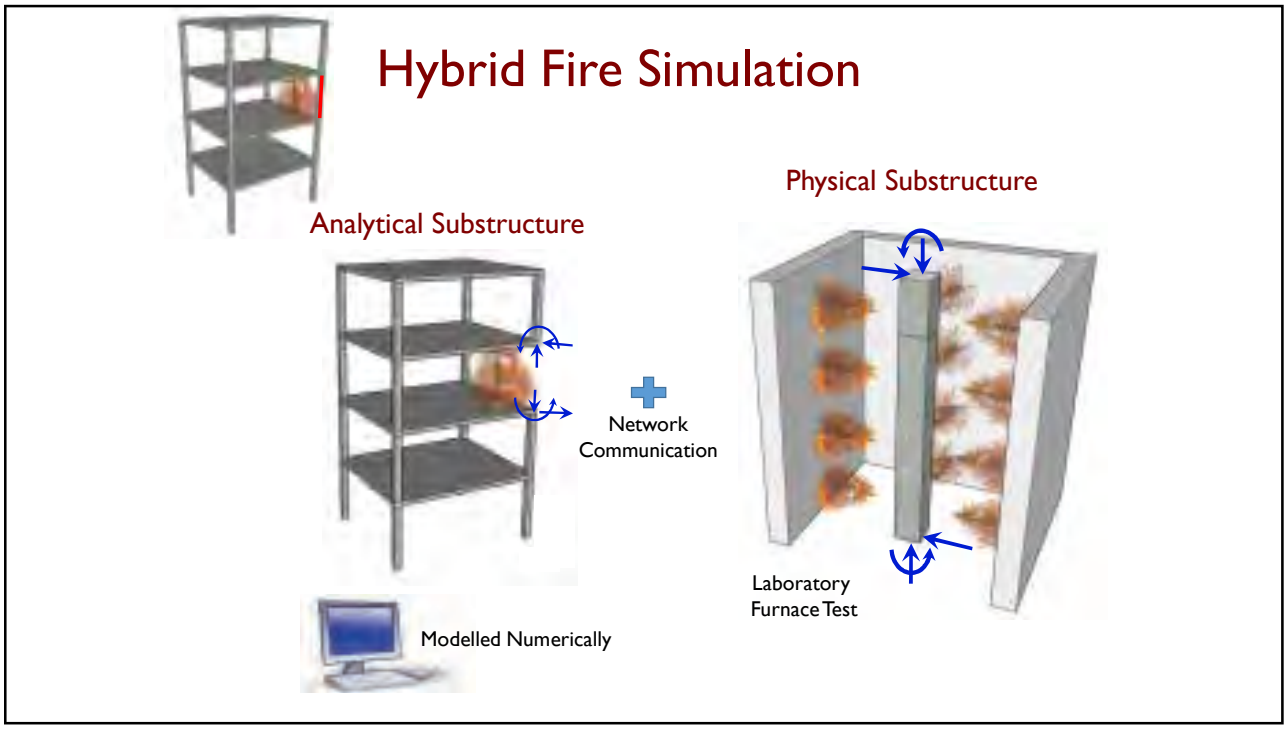

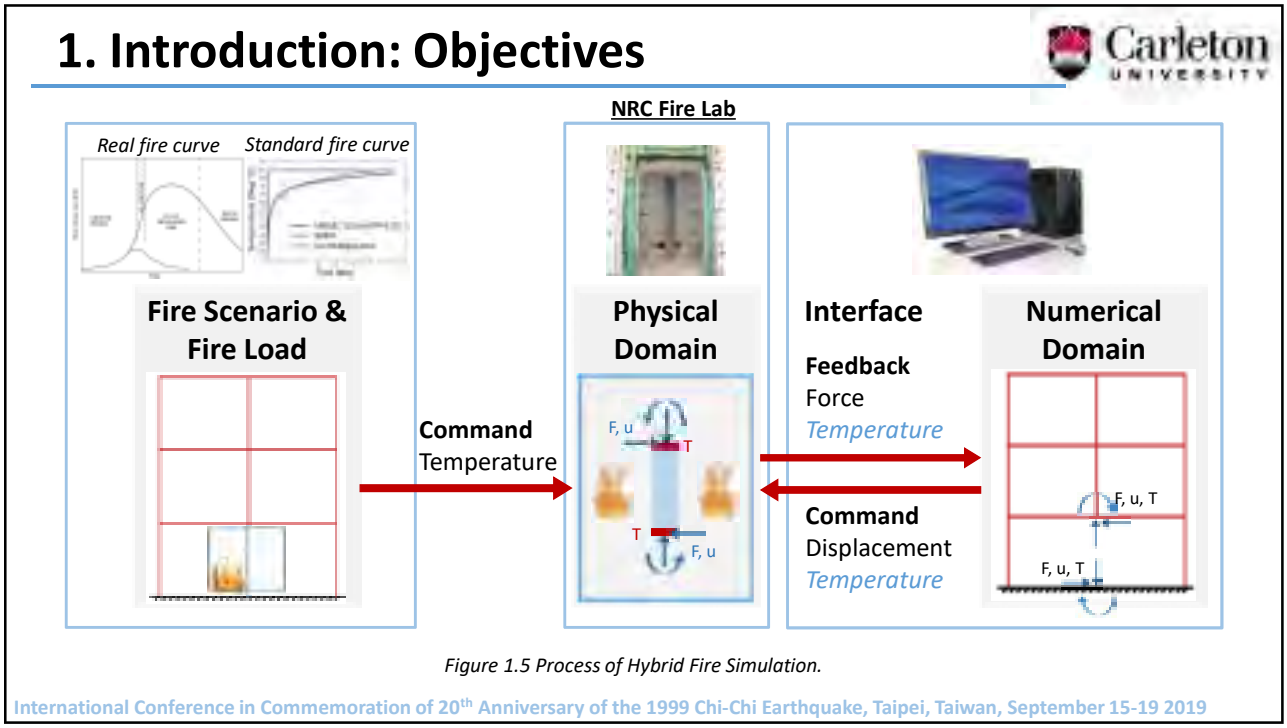

Figure 1.5 Process of Hybrid Fire Simulation.

2. Background and Literature Review

Fire Exposure:

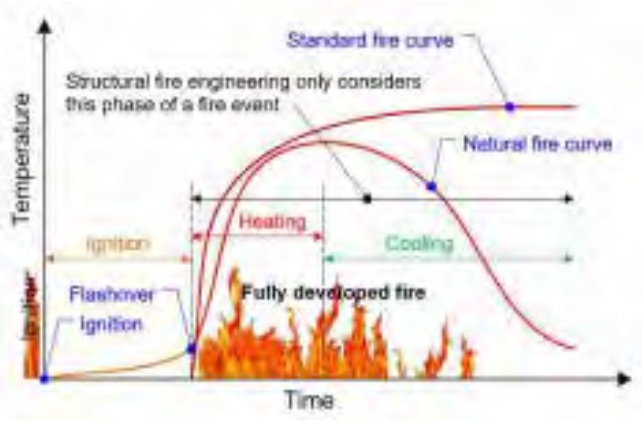

Figure 2.6 Typical time-temperature curve for fire in compartment (Buchanan, 2017).

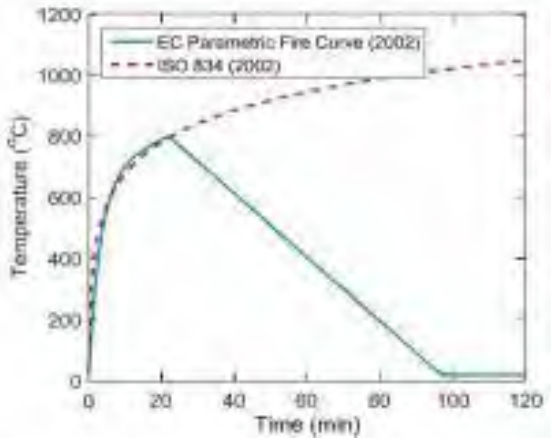

Figure 2.7 A comparison between ISO 834 (CEN, 2002) standard fire curve and Eurocode parametric fire curve (CEN, 2002) assuming Γ=1.0. (Memari, 2016).

2. Background and Literature Review

Previous Research	Structure	Testing Facility	Physical Domain	Interface	MDOF	TDOF	Numerical Domain	Heat Conduct to Adjacent Compenents
Kerzen et al. (1999)	8-storey steel frame	Gas Furnace (BAM)	Single column	6-channel control system	1 (axial)	--	Constant axial stiffness	--
Robert et al. (2010)	1-storey concrete frame	Gas Furnace (CERIB)	Single slab	--	3 in total (1axial+ 2rotational)	--	Constant stiffness	--
Mostafaei (2012)	6-storey reinforced concrete frame	Gas Furnace (NRC)	Single column	Human interaction	1 (axial)	--	SAFIR 2D/3D (nonlinear)	--
Whyte et al. (2014)	steel truss	Electric Furnace (ETH)	Single truss	OpenFresco/New objects for truss element	1 (axial)	1	OpenSees/Standard (linear)	--
Schnabl et al. (2016)	steel truss	Electric Furnace (ETH)	Single truss	Server	1 (axial)	--	ABAQUS (user subroutine)	--
Wang et al. (2018)	4-storey steel frame	Gas Furnace (KIST)	Single column	UT-SIM	1 (axial)	--	ABAQUS (nonlinear)	Predefined time-temperature curve

International Conference in Commemoration of 20th Anniversary of the 1999 Chi-Chi Earthquake, Taipei, Taiwan, September 15-19 2019

3. Proposed Framework for Hybrid Fire Simulation

Mechanical and thermal data full exchange:

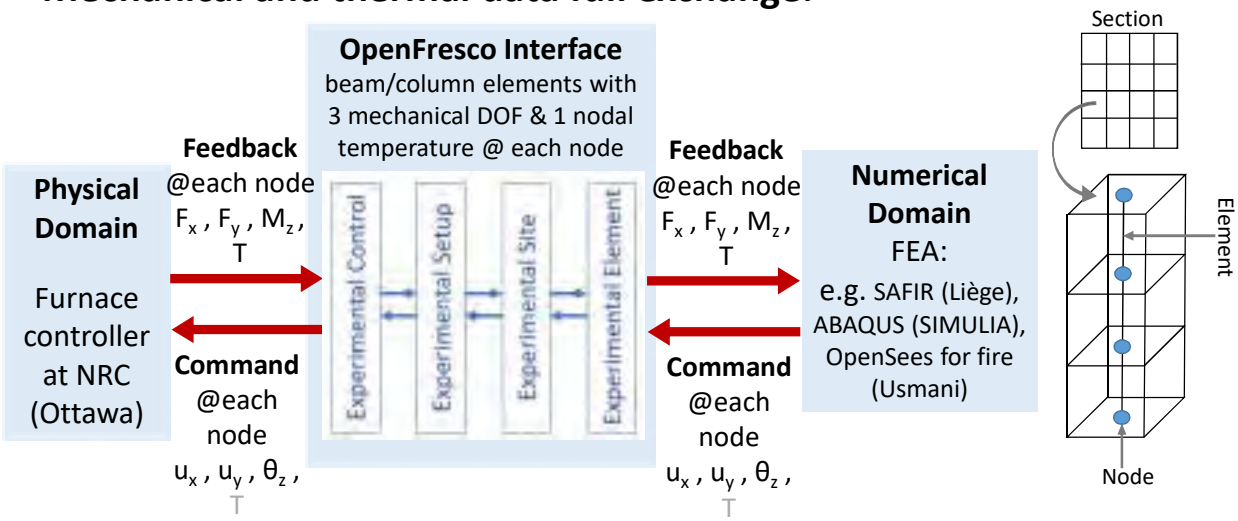

Figure 3.1 Proposed hybrid fire simulation framework.

4. Example of Hybrid Fire Simulation of a Steel Building

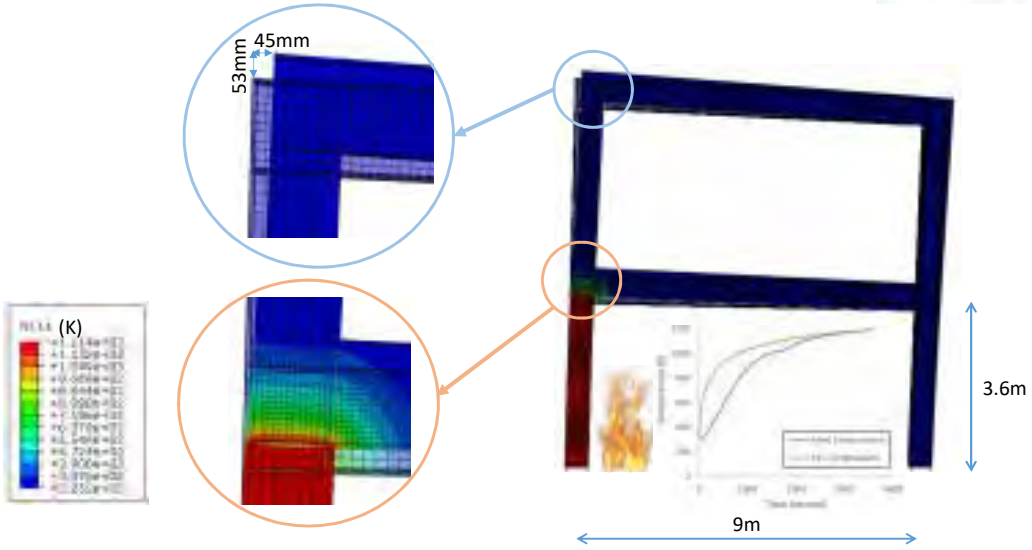

Figure 4.1 Prototype steel frame subjected to elevated temperature.

4. Example of Hybrid Fire Simulation of a Steel Building

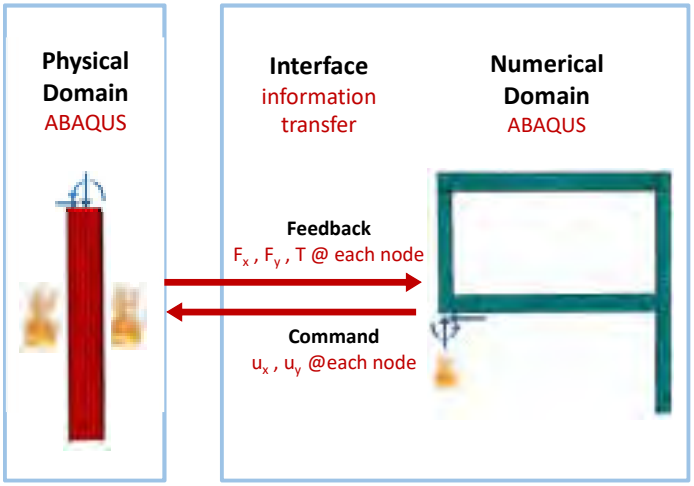

Figure 4.3 Process of the demonstration example.

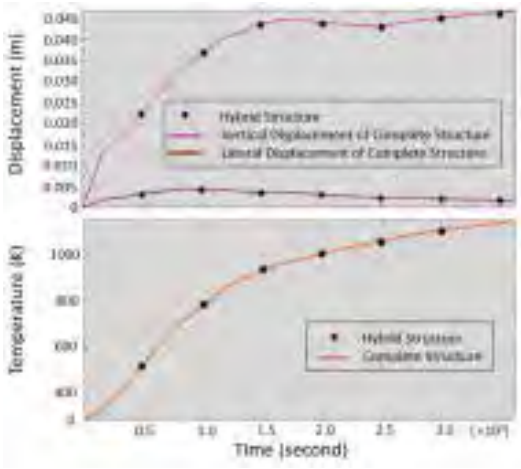

Figure 4.4 Displacement and temperature at one interface node of the complete model and hybrid model.

5. Performance of a Steel Building under Fire Following Earthquake

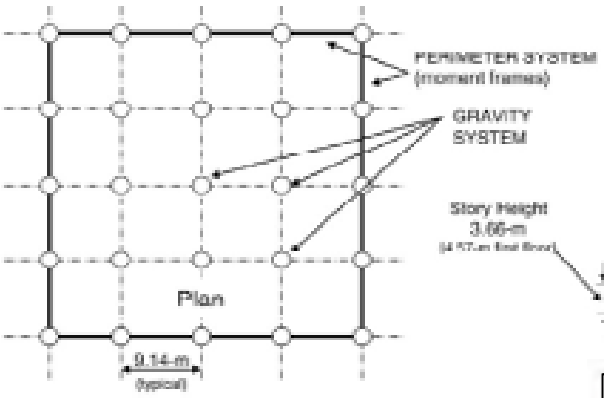

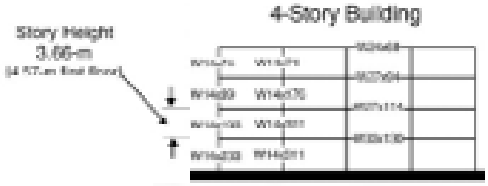

Figure 5.1 Design details of the prototype structure (Jin and El-Tawil, 2004).

Mode number	1	2	3	4
Period (second)	1.08	0.39	0.23	0.14
Frequencies (Hz)	0.93	2.55	4.44	7.2

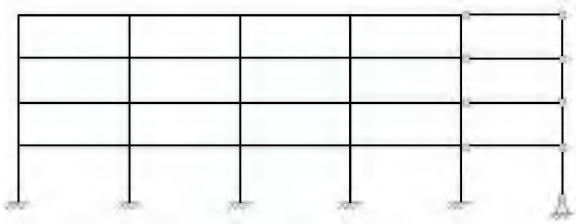

Figure 5.2 Configuration of the numerical model in ABAQUS.

5. Performance of a Steel Building under Fire Following Earthquake

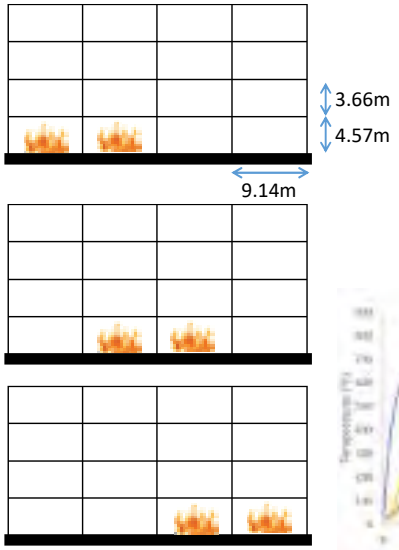

Figure 5.3 Prototype structure and fire scenarios.

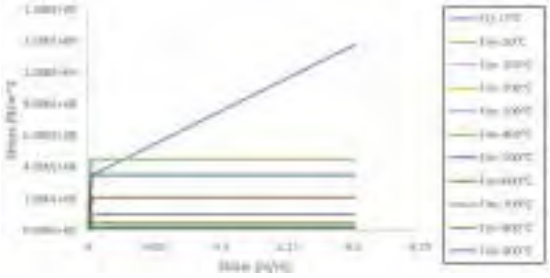

Figure 5.4 Material properties for earthquake and fire analysis.

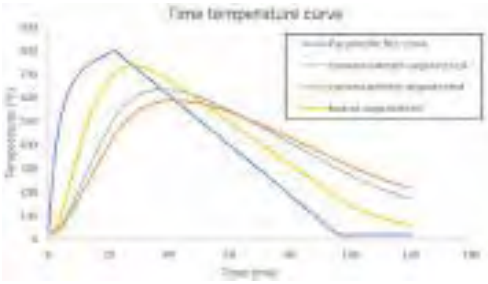

Figure 5.5 Temperature history for different sections.

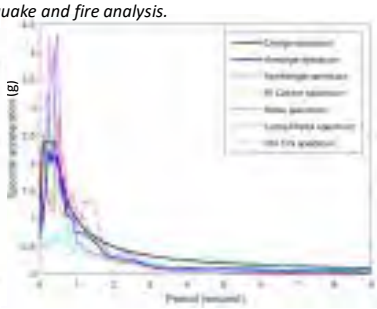

Figure 5.6 Seismic response spectrum.

5. Performance of a Steel Building under Fire Following Earthquake

Effect of post-Kobe-earthquake fire in element sections:

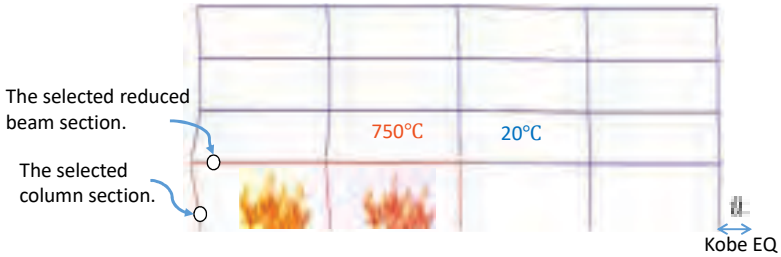

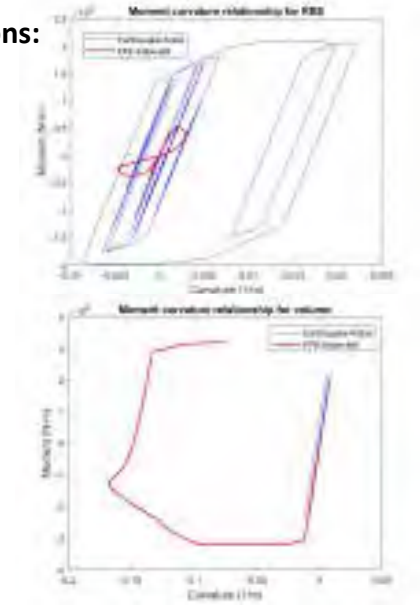

6. Conclusions and Future Research

- **Potential to Consider Fire Spread Scenarios by using multiple furnaces or multi-site test.**

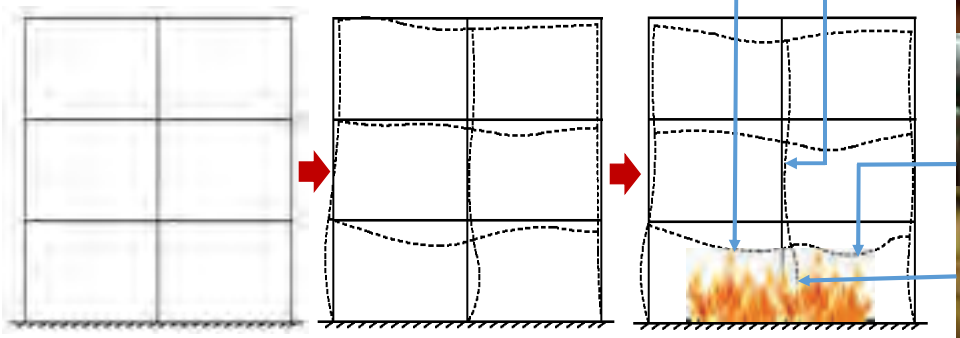

2D steel frame subjected to fire.

Geographically distributed furnace.

Wall furnace at another lab.

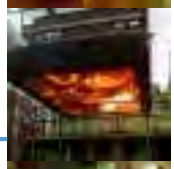

Floor furnace at NRC.

Column furnace at NRC.

Summary

Fire following earthquake hybrid simulation is a promising approach:

- **To provide a reliable and cost-effective tool alternative to full-scale tests;**
- **To consider fire spread scenarios;**
- **To conduct parametric studies.**

Thank You!

Acknowledgements:

- Canadian Foundation for Innovation (CFI)
- NSERC
- Francois Forcier, Drs. Shawn You and Shawn Gao at MTS
- Martin Leclerc at Ecole Polytechnique Montreal
- Professor YS Yang at Tapei Tech
- Nordic Structures

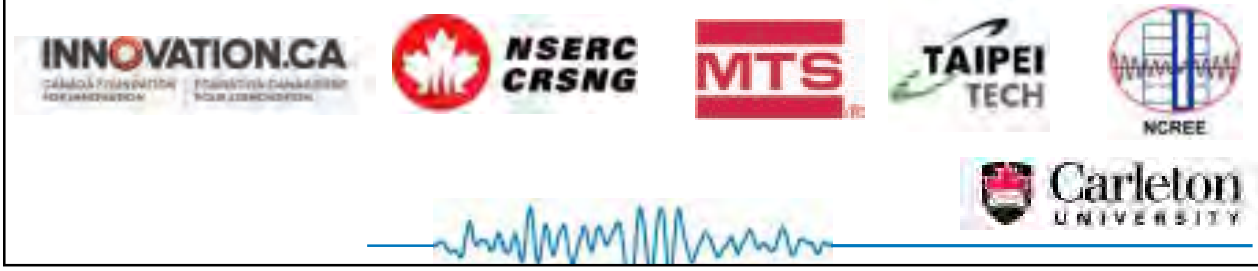

US-TAIWAN COLLABORATIVE RESEARCH ON STEEL COLUMNS: CYCLIC LATERAL TESTING OF TWO-STORY SUBASSEMBLAGES

By Dr. C.-C. Chou, National Taiwan University/ National Center for Research on Earthquake Engineering (NCREE)

Abstract

The investigation is an on-going cooperative research program among the NTU, UC, San Diego, UM, Ann Arbor, and NCREE. The work is funded by MOST, Taiwan and NIST, USA. The objective of this research is to study the seismic performance of first-story steel columns under combined axial load and cyclic lateral drifts. To reflect realistic boundary conditions, four half-scale, two-story steel subassemblage frames with a single column and steel beams extending half the bay length at the second and third stories were designed for testing to evaluate the cyclic behavior of steel columns. The first subassemblage test was conducted during the Conference in Commemoration of 20th Anniversary of the 1999 Chi-Chi Earthquake, Taiwan. The test showed that although the column satisfies the compactness requirement of the highly ductile member per AISC Seismic Provisions (2016), the column under medium axial load cannot deliver plastic rotation of 0.03 rad. in the subassemlage.

Keywords: H-shaped column, welded-box column, compactness, column boundary condition, two-story subassemblage frame test.

Biography

Dr. Chung-Che Chou is a Professor in Department of Civil Engineering, Vice Dean of Faculty of Engineering, National Taiwan University (NTU), and the Head of Building Engineering Division of NCREE. He received his Ph.D. degree in 2001 from the University of California (UC), and then worked as an Assistant Project Scientist for the New San Francisco-Oakland Bay Bridge project. His research interests include steel structure, composite structure, earthquake-resisting design, large-scale structural testing and structure retrofit.

NTU, UCSD, UM, NCREE

NARLabs

US-Taiwan Collaborative Research on Steel Columns: Cyclic Testing of Two-Story Subassemblages

Chung-Che Chou, Te-Hung Lin, Hou-Chun Xiong, Yun-Chuan Lai
Chia-Ming Uang, Sherif El-Tawil, Jason P. McCormick, Gilberto Mosqueda

National Taiwan University, University of California, San Diego
University of Michigan, Ann Arbor, National Center for Research on Earthquake Engineering

承諾・熱情・創新

NRC-MOST WORKSHOP
Oct. 7-9, 2019, Canada

www.narlabs.org.tw
cechou@ntu.edu.tw

NARLabs

Column Tests with Fixed End

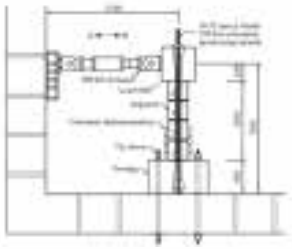

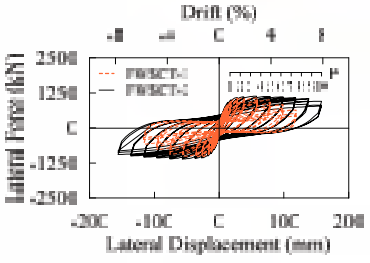

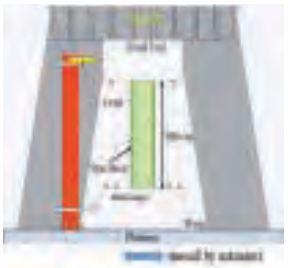

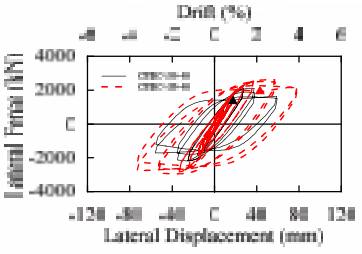

Chou and Chen (2006) EESD; Chou et al. (2018) Const. & Building Mat.; Chou & Wu (2019) Engrg. Struct.

2

NARLabs

DC-SCBF and BRBF Test

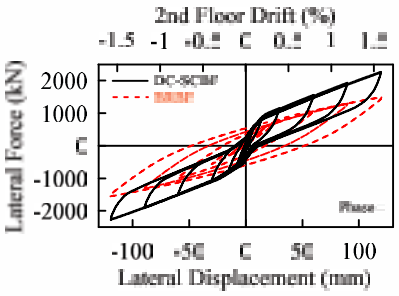

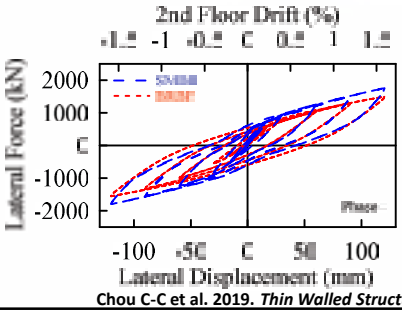

Chou C-C et al. 2019. *Thin Walled Structures*

NARLabs

Sandwiched BRB

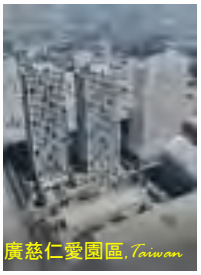

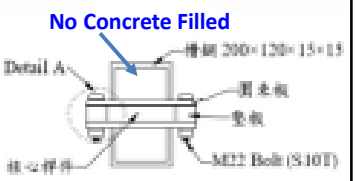

C_{max}/T_{max}<1.06

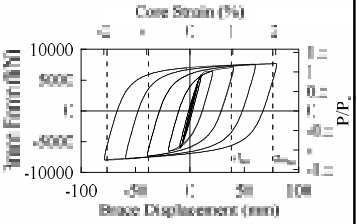

Chou & Chen 2010. *Engrg. Struct.*
Chou & Liu 2012 *Earthquake Spectra;*
Chou et al. 2012 *Earthq. Engrg. Struct. Dyn.*
Chou et al. 2016. *Engrg. Struct.*

4

NARLabs

Dual-Core Self-Centering Brace

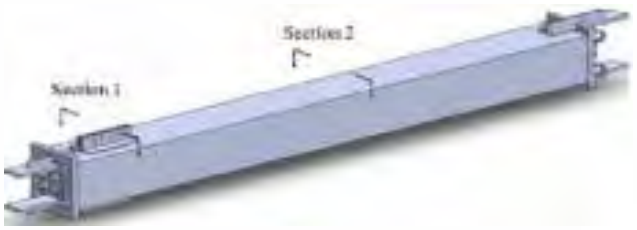

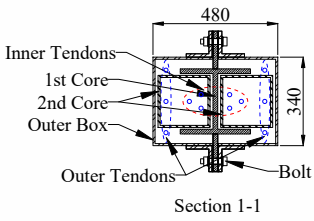

DC-SCB

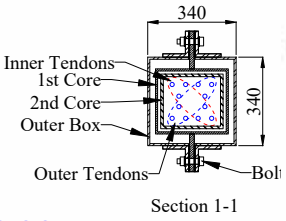

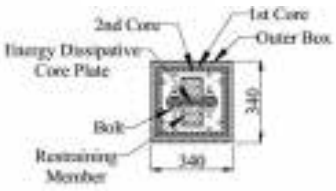

SC-SBRB

Chou et al. 2016. Engre. Struct.; Chou and Chen. 2015. *Earthquake Spectra*
Chou et al. 2014. Engrg. Struct.; Chou and Chung 2014. J. Const. Steel Res.

NARLabs

Large-Scaled DC-SCB Test

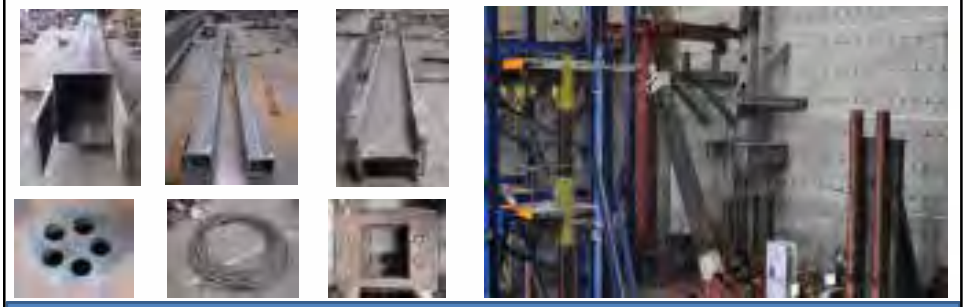

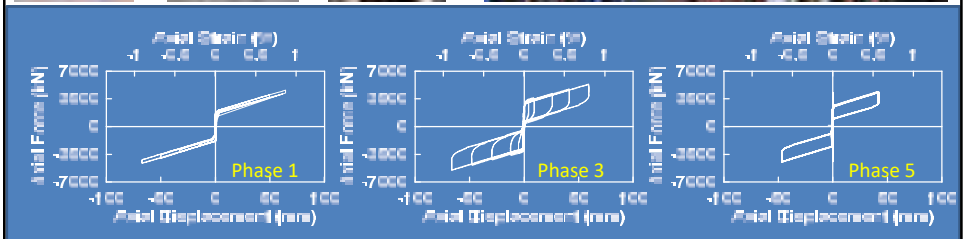

Chou et al. 2016. *Engineering Structures*

NARLabs

Objectives

- Study the seismic performance of first-story steel columns under axial load and cyclic lateral drift with realistic boundary conditions.
- Subassemblage specimens represent a bottom portion of the prototype.
- Funded by MOST, Taiwan and NIST, USA

7

NARLabs

Prototype and Subassemblage

- **Prototype Frame**

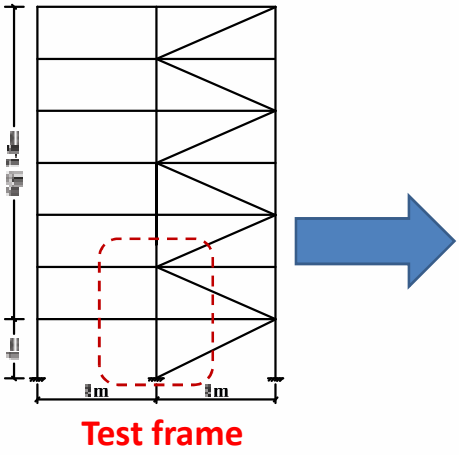

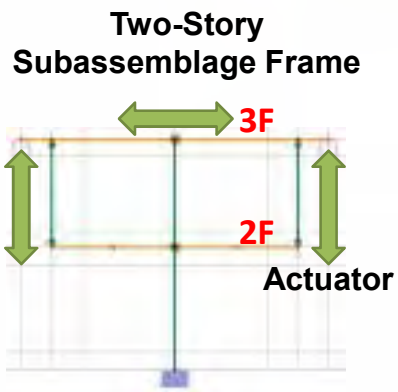

NARLabs

Ground Motion

■ Time History Analysis

Event	Type	Year	Station	PGA (gal)	PGV (cm/sec)	Scaled PGAs (gal)
Kobe	Far field	1995	ABN090	230	24	1098
Landers	Near fault	1992	Lucerne-260	711	134	1203

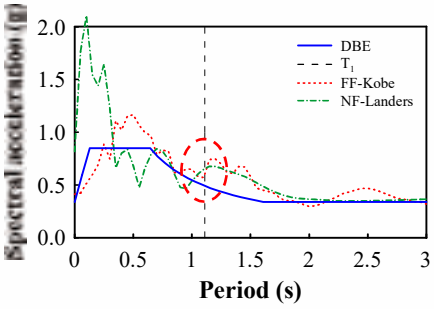

MCE level

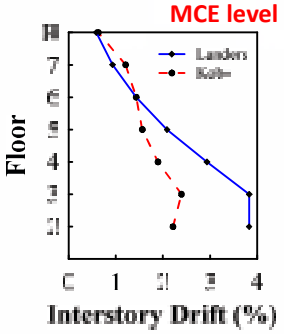

9

NARLabs

Test Setup Validation

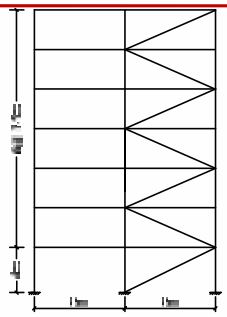

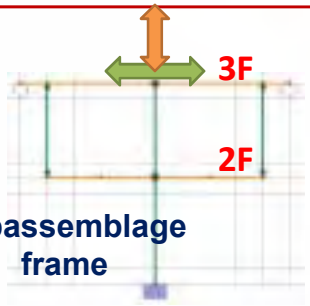

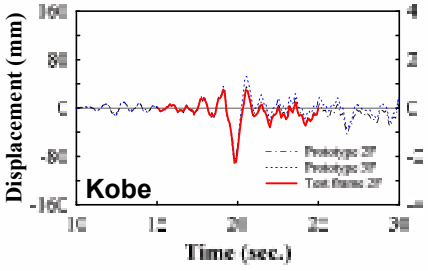

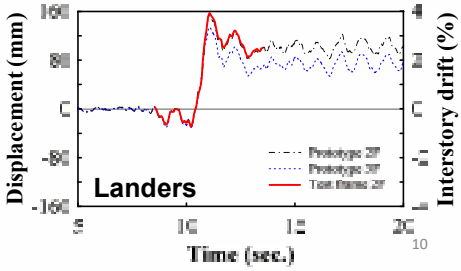

10

NARLabs

Landers Earthquake

■ First-Story Center Column

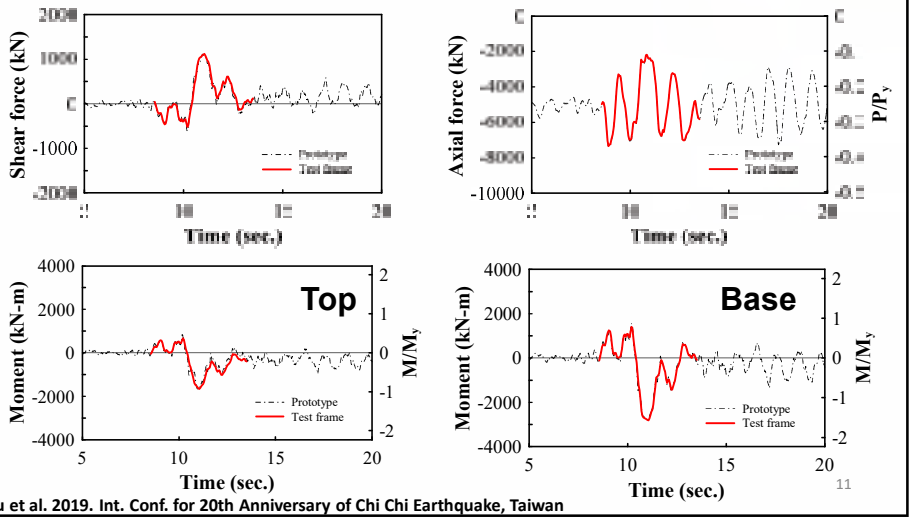

Chou et al. 2019. Int. Conf. for 20th Anniversary of Chi Chi Earthquake, Taiwan

NARLabs

Two-Story Subassemblage

First Test Conducted in Int. Conf. for 20th Anniversary of Chi-Chi Earthquake, Taiwan, September 2019

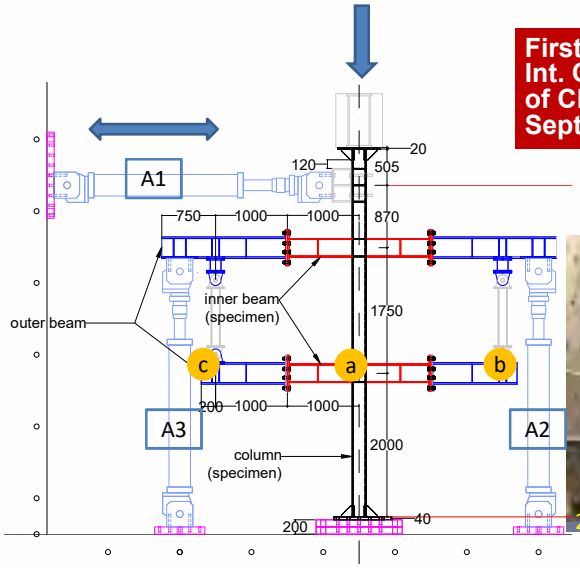

NARLabs

Test Matrix

	Specimen 1	Specimen 2	Specimen 3	Specimen 4
Section	Box Column 190X190X13	Box Column 230X230X13	H-shaped Column 320X160X8X12	H-shaped Column 320X160X6X12
b/t (Flange)	12.61	15.69	6.67	6.67
b/t (Web)	12.61	15.69	37	49.3
Material	SM570MB	SM570MB	SN490B	SN490B
Axial force / P_y	0.4	0.4	0.2	0.2

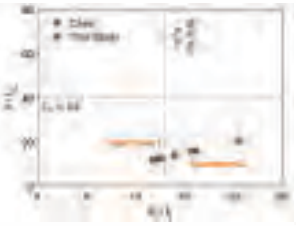

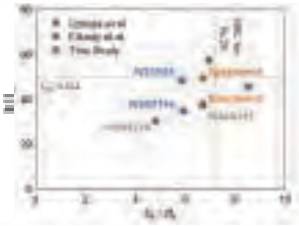

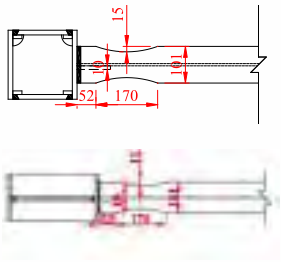

NARLabs

Two-Story Subassembalge

NARLabs

Test Response

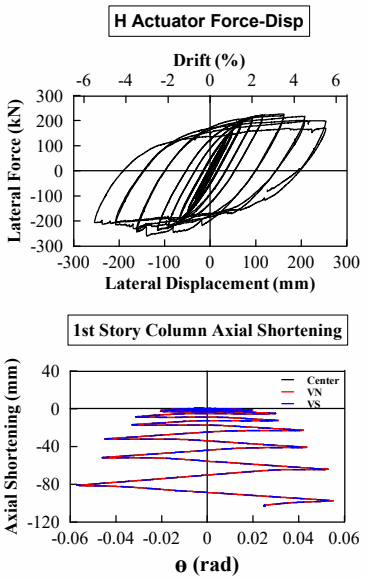

NARLabs

Free-Body Diagram

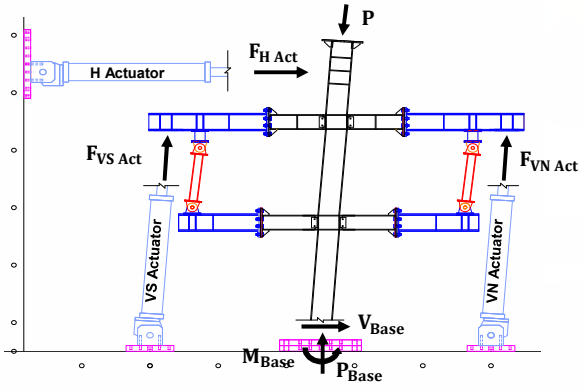

$$M_{Base} = \left[L_{H\,Act}(F_{H\,Act}\cos\theta_{H\,Act}) - (L_{H\,Act} + L_{Top})(P\sin\theta_{Top})\right] + \left[P\cos\theta_{Top}\delta_{H\,Act} + F_{H\,Act}\sin\theta_{H\,Act}\left(\delta_{H\,Act}\frac{L_{Act} + L_{Top}}{L_{Act}}\right)\right] + \left[(L_{3F\,B}\cos\theta_{VS\,Act})F_{VS} - (L_{3F\,B}\cos\theta_{VN\,Act})F_{VN}\right]$$

NARLabs

Axial Force and Moment of Column

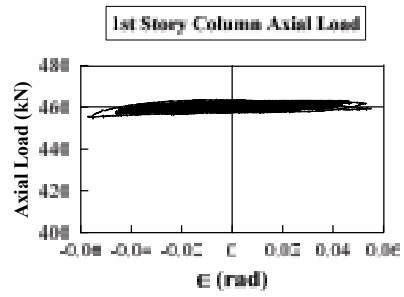

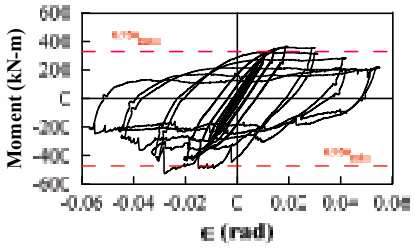

Section Comparison

Section	Material	$b_f/2t_f$	h/t_w	L/r_y
Specimen3	SN490B	6.67	37	55.2
W24X131	A992	6.7	37.3	72.7

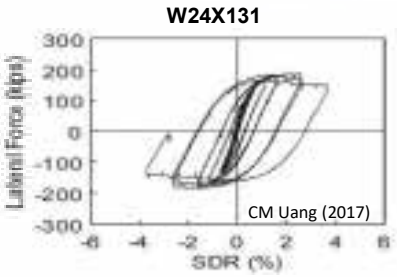

NARLabs

Conclusions

The column that satisfies AISC requirement (2106) does not perform well after 3% drift, lower than 90% peak strength.

The column carries axial load throughout the test although the column experiences significant local buckling at drift of 5%. The force redistribution after column buckling is effective to maintain strength of the subassemblage.

NARLabs

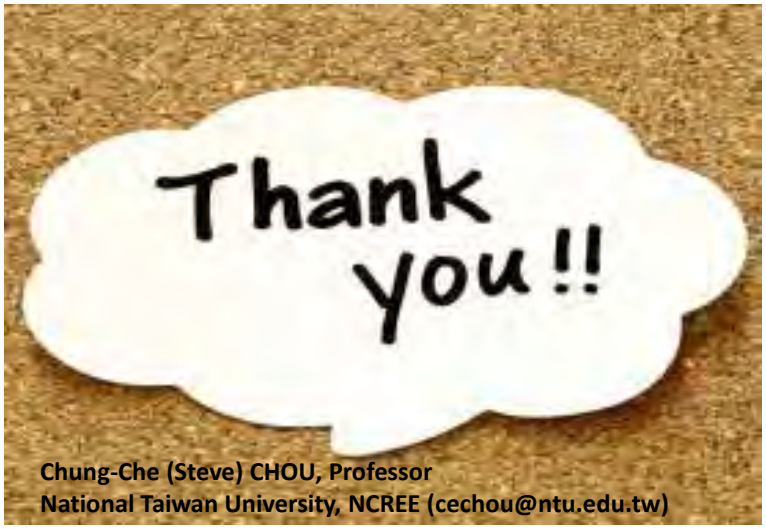

Chung-Che (Steve) CHOU, Professor
National Taiwan University, NCREE (cechou@ntu.edu.tw)

DEFORMATION CAPACITY OF RC STRUCTURAL MEMBERS AND DEFINITION OF ACCEPTANCE CRITERIA - A REVIEW OF THE NEW EUROCODE 8-I (2020)

By Dr. S. J. Pantazopoulou, York University

Abstract

The revised version of Eurocode 8-1 (Seismic Design) and 8-3 (Retrofit) to be released in 2022 brings forth a number of open issues related to seismic design, concerning the implementation of the state of the art in terms of improved estimations of both demand and supply, with an emphasis on deformation measures. These include revisions in the R-μ-T relationships, revised performance level definitions in terms of milestone values of member drift ratio, consideration of cyclic degradation for long duration motion and revised stability indices. The results, obtained from analysis of model structural components using IDA with pertinent ground motions, address the core assumptions of seismic design (e.g. the equal displacement rule). At the same time, research has been going on towards improved understanding of the sequence of failure in structures and how this affects the dependable deformation capacity that is used in the acceptance criteria. In this context, revised expressions are developed for the plastic hinge length in reinforced concrete structural members considering the strain penetration effects, and the implication thereof on rotation capacity is evaluated. The relevance of material strain limits used instead of drift ratio in some codes as predictors of member performance, in light of the residual deformations occurring during cyclic displacement reversals, is discussed with reference to the different approaches used in the European and Canadian codes.

Keywords: rotation capacity, acceptance criteria, performance indices, response modification, ductility.

Biography

Dr. S.J. (Voula) Pantazopoulou holds a University Civil Engineering Diploma from the National Technical University of Athens, and M.Sc. and Ph.D. degrees from the University of California (UC), Berkeley. She has worked for 31 years as a faculty member at the University of Toronto (1988-1998), Democritus University of Thrace (1998-2011) and the University of Cyprus (2011-2015). She resumed her career at York University in Canada in 2016. Her research interests include seismic design, assessment and retrofit of structures and bridges with innovative structural materials.

Deformation Capacity of R.C. Structural Members and Definition of Acceptance criteria - a Review of the New EN 1998 (2020) (Eurocode 8 -1, -3)

S. J. Pantazopoulou, Professor of Civil Engineering
York University, Toronto, Ontario, Canada

Emerging new version of EC8 – 2020:

Near Collapse (NC): heavy damage, large permanent drifts, retains its vertical-load bearing capacity; most ancillary components, where present, have collapsed.

Significant Damage (SD): significant damage, moderate permanent drifts, retains its vertical-load bearing capacity; ancillary components, where present, are damaged (e.g., partitions and infills have not yet failed out-of-plane). Repairable, but, may be uneconomic.

LS of Damage Limitation (DL): slight damage, economic to repair, negligible permanent drifts, undiminished ability to withstand future earthquakes and structural members retaining their full strength with a limited decrease in stiffness; (partitions and infills may show distributed cracking).

Fully Operational LS (OP): slight damage, economic to repair, structure remains in continuous operation.

Performance objectives ➔ Indicators of Damage

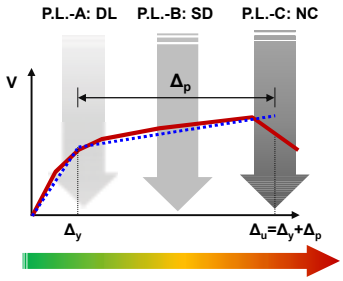

Limit state:	Max. Displ.	Cost of repair/replace
Damage Limitation: Operational: A1	Δ_y	0%-10%
Damage Limitation: Immediate Occupancy: A2	$\Delta_y+0.3\Delta_p$	5%-30%
Significant Damage – Life safe: B	$\Delta_y+0.6\Delta_p$	20%-50%
Near Collapse: C	$\Delta_y+\Delta_p$	>70%

Limit State linked to Event Return Period

Return Periods of Seismic Action in Years

Limit State	Consequence Class			
	CC1	CC2	CC3-a	CC3-b
NC	800	1600	2500	5000
SD	250	475	800	1600
DL	50	60	60	100

- **Point of reference for strength: SD Limit State**
- **Use Capacity Design Principles to avoid Brittle and Unstable Failure**
- **Deformation Capacity classified in DC1, DC2, DC3**

Range of $S_{a,475}$(m/s²) values to define seismicity levels

Seismicity Level	$S_{a,475}$ (m/s²)
Very Low	< 1.0
Low	1.0 – 2.5
Moderate	2.5 – 5.0
High	>5.0

Seismic action effects in the structure evaluated using two alternatives:

(1) The **force-based** approach: linear analysis, nonlinearity considered using Response Modification Factor
Force-based approach cannot be used for verification of the NC limit state.
Displacement demands calculated through R-μ-T relationships

(2) The **displacement-based** approach: non-linear static analysis based on pushover calculation, IDA, on NTHA.
Displacements obtained directly from the analysis

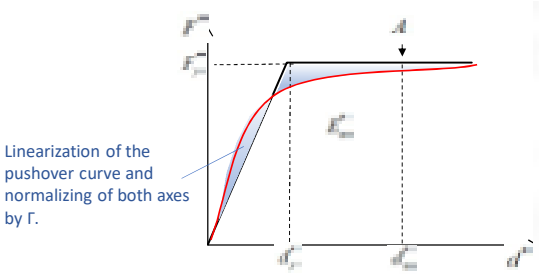

Linearization of the pushover curve and normalizing of both axes by Γ.

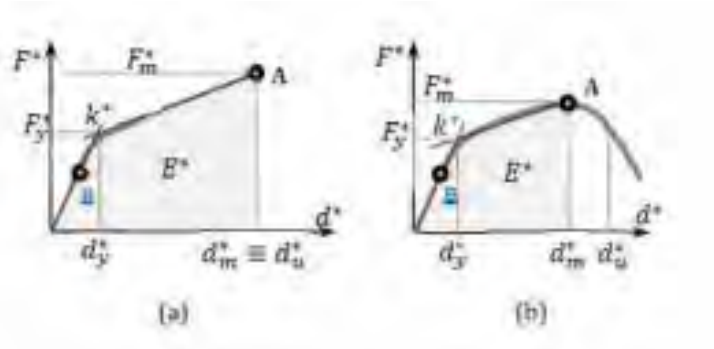

Gravitational Field in the Direction of Sway

Calculate the fundamental period of vibration and associated mode from

$$T = 2\sqrt{\frac{m_i \cdot s_i^2}{m_i \cdot s_i}}$$

g = 9.81m/s²

s_i are displacements obtained from the gravitational field applied in the horizontal direction

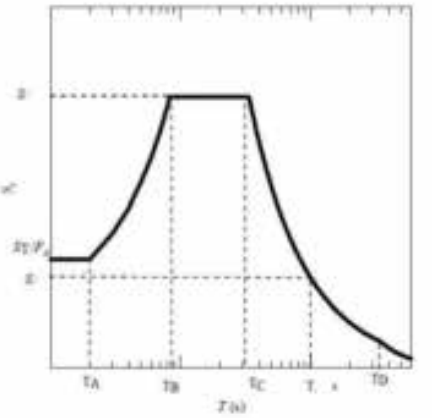

$$S_d = S_e(T) \cdot \frac{T^2}{4\pi^2}$$

Elastic Displacement Demands

$$S_d(T) = S_d(T_E) \times \left[1 + \left(\frac{F_L}{F_\beta} - 1\right)\right] \cdot \frac{T - T_E}{T_F - T_E}$$

max(T_D; 6s)

T_F = 10s

Long period amplification

Effect of Duration on Demand Estimation on Systems with degrading properties

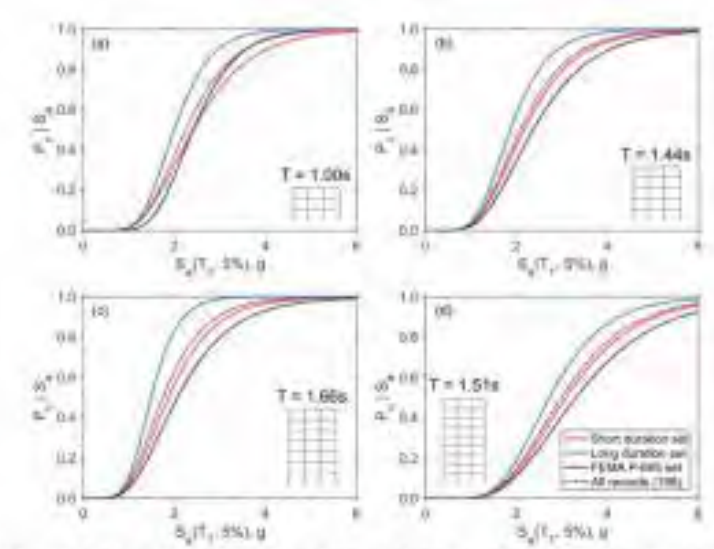

Figure 8 Collapse fragility curves for frames: a) 3-storey, b) 5-storey, c) 7-storey, d) 9-storey

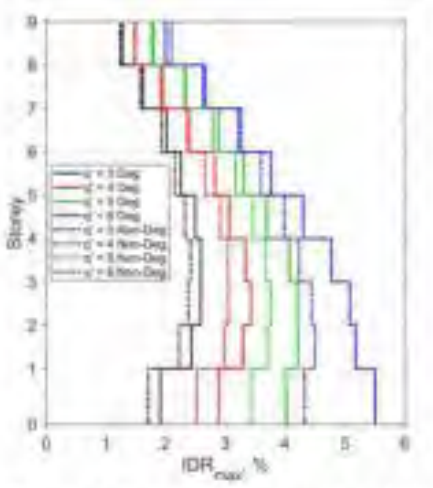

Figure 5 Distribution of median θ_{mod}

Effect of Duration on Demand Estimation

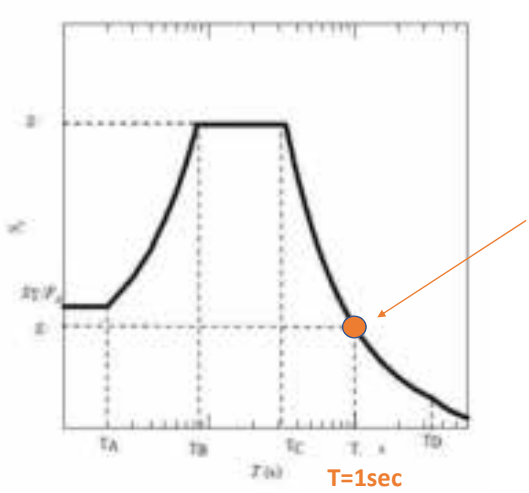

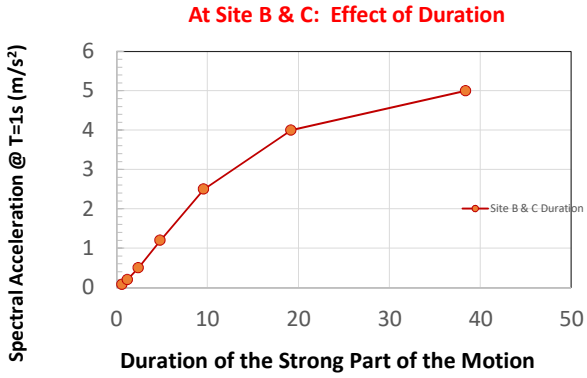

Modification of the R-μ-T relationships

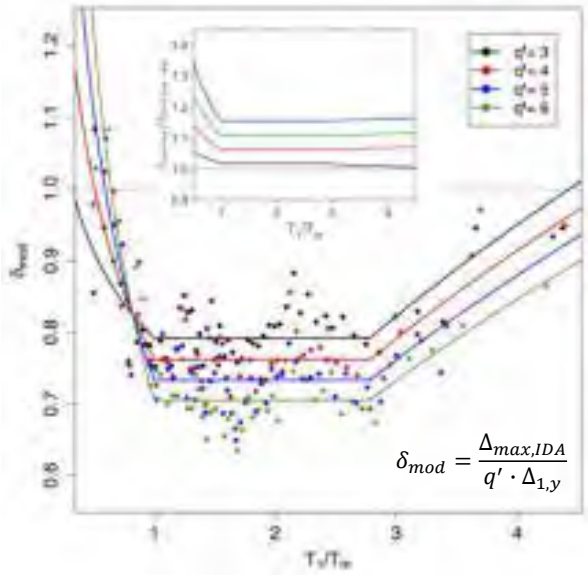

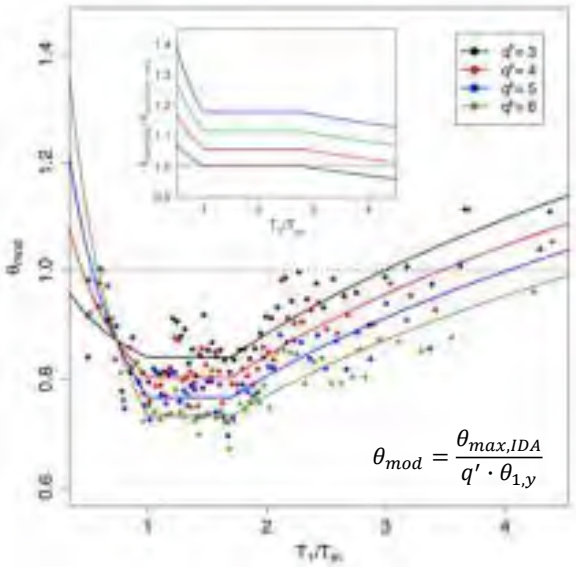

Mean Period (Tm): weighted mean of periods of the Fourier Amplitude Spectrum (FAS) over a pre-defined frequency range, where the weights are assigned based on the Fourier amplitudes.

Deformation Capacity of Structural Elements

- **Drift capacity estimations and Shear Strength estimations for new Designs, are obtained using the same methodologies as in the case of Seismic Assessment**

Drift limitation at SD applies to all ductility classes.

$$\mathbf{d_{SD} = d_y + \frac{0.5}{\gamma_{Rd,SD}} \cdot (d_u - d_y)}$$

Verification at NC: $\mathbf{d_{NC} = d_y + \frac{1.0}{\gamma_{Rd,SD}} \cdot (d_u - d_y)}$

Verification at DL: $\mathbf{d_{DL} = d_y}$

- **Drift < 0.3% - 0.5% for structures with masonry ancillary elements attached to the structural;**
- **<0.7% for structures with ductile ancillary elements, and**
- **<1% if the ancillary elements are not attached to the structural components.**

Strain Displacement Transformations

Local – to – Global transformations

$$\Delta_y^{fl} = \frac{1}{3}\varphi_y L_s^2 \qquad \Delta_p^{fl} = (\varphi_u - \varphi_y)\ell_p(L_s - 0.5\ell_p)$$

$$\Delta_y^{sh} = \frac{V_c}{0.4 \cdot E_c \cdot 0.8A_g} \cdot L_s \qquad \Delta_p^{sh} = \varepsilon_{st} \cdot L_s = \frac{Vc_{u,\lim}}{E_s \sum_i A_{sw_p}}$$

$$\Delta_y^{sl} = \frac{\varphi_y \cdot D_b}{8} \cdot \frac{f_y}{f_{b,y}} \cdot L_s \qquad \Delta_p^{sl} = (\varphi_u - \varphi_y) \cdot \frac{D_b}{4} \cdot \frac{\beta f_u}{f_{b,u}} \cdot L_s$$

$$\varphi = \frac{\varepsilon_s}{d-c}; \quad \varphi_u = \frac{\varepsilon_{c,u}}{c}$$

$$0 < \beta = (f_u - f_y)/f_u < 0.5$$

$$\ell_p = \beta L_s + \frac{D_b}{4} \cdot \frac{\beta}{(1-\beta)} \cdot \frac{f_y}{f_{b,u}} + z$$

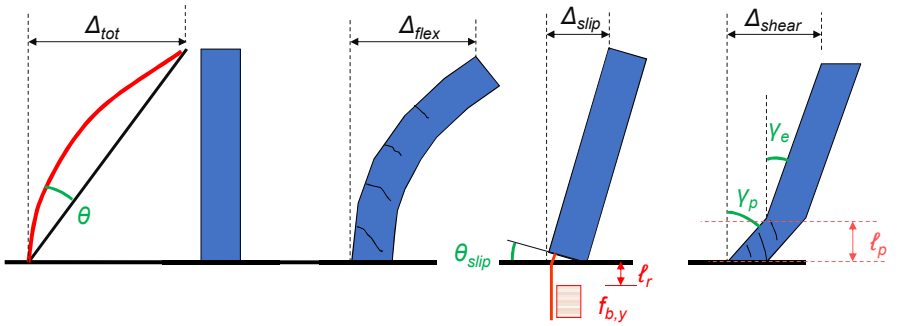

Consider depth of yield penetration, ℓ_r

Deformation Capacity of Structural Elements

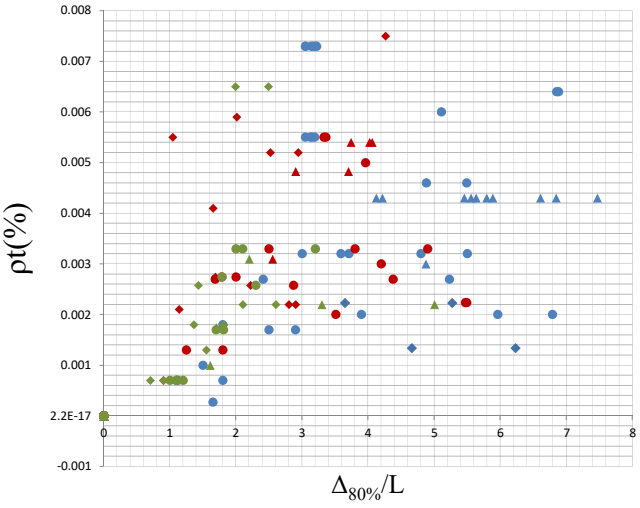

- Aspect Ratio(a/D<2)
- Aspect Ratio((2<a/D<4))
- Aspect Ratio(4<a/D<8)

v<0.15

- Aspect Ratio(a/D<2)
- Aspect Ratio((2<a/D<4))
- Aspect Ratio(4<a/D<8)

0.15<v<0.3

- Aspect Ratio(a/D<2)
- Aspect Ratio((2<a/D<4))
- Aspect Ratio(4<a/D<8)

0.3<v<0.6

Deformation Capacity of Structural Elements: new approach merges columns, beams, walls; new design & assessment

$$EI = \frac{M_y}{\theta_y} \cdot \frac{L_s}{3} \qquad \theta_y = \varphi_y \cdot \frac{L_s + a_V(d - d')}{3} + 0.0019 \cdot \left(1 + \frac{h}{1.6L_s}\right) + \varphi_y \cdot \frac{D_b f_y}{8\sqrt{f_c}}$$

$\theta_{y,flex}$ $\theta_{y,shear}$ $\theta_{y,anchor}$

0.0011 for walls

0.0025 for walls (1-(L_v/8D) for circular piers

a_V=0 for $V_{flex}<V_c$; otherwise, a_V=1

For lapped reinforcement, ε_y & f_y are obtained by mult. by $L_{d,avail}/L_{d,min}$:

$$f_s = f_y \cdot \left(\frac{L_{d,avail}}{L_{d,min}}\right); \quad \frac{L_{d,min}}{D_b} = \frac{f_y}{3.3\sqrt{f_c}};$$

If $V_{flex} > V_{shear}$, θ_y reduced by mult. by V_{shear}/V_{flex}.

Deformation Capacity of Structural Elements

$$\theta_{pl} = \kappa_{conform} \cdot \kappa_{axial} \cdot \kappa_{long-reinf} \cdot \kappa_{concrete} \cdot \kappa_{aspectratio} \cdot \kappa_{confinement} \cdot \theta_o^{pl}$$

1 for Conf, or 0.78 for NConf

0.2^{ν}

$\left[\frac{\max(0.01, \omega')}{\max(0.01, \omega_{tot} - \omega')}\right]^{0.25}$

$(f_c/25)^{0.1}$

Reference Value of Aspect ratio = 2.5, f_c=25MPa, v=0:

3.9% beam, or rect. Column

2.3% rect. Wall

2.7% Barbell Wall, or Box Section

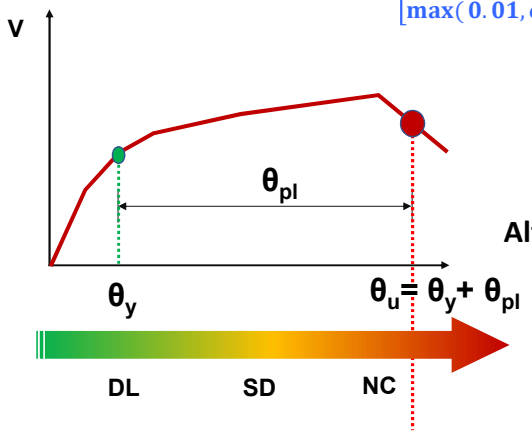

End of an element: @80% of peak load

Alternatively, Calculate from Basics, Using L_p Estimation

$$\theta_{pl} = (\phi_u - \phi_y) \cdot L_{pl} \cdot \left(1 - \frac{0.5L_{pl}}{L_v}\right) + 9.5 \cdot D_b \cdot \frac{\phi_u - \phi_y}{2}$$

$$L_{pl} = \lambda_{section} \cdot \lambda_{shearspan} \cdot \lambda_{axial} \cdot (0.3h)$$

Curvature Capacity ϕ_u, and ϕ_{pl} depend on critical event at failure

Some Examples of Critical Events:

- Cover Delamination (i.e., $\varepsilon_{c,2}$ in cover ≥ 0.0035-0.005).
- Exceeding compression strain capacity of confined core: $\varepsilon_{c,c2} > \varepsilon_{c,cu}$.
- Loss of concrete contribution component to lap-splice strengths (splitting along lap) (under cyclic reversals it occurs at longitudinal compressive strain $\varepsilon_{c,c2} > 0.002$).
- Exhaustion of reinforcement anchorage strain development capacity owing to yield penetration: $\varepsilon_{s,1} \geq min\{\varepsilon_{s,anch}; \varepsilon_{s,u}\}$ ($\varepsilon_{s,anch}$ is the strain capacity of the anchorage or lap; $\varepsilon_{s,u}$ is the fracture strain of the reinforcement).
- Buckling / instability of compressive longitudinal reinforcement: $\varepsilon_{s,2} > \varepsilon_{s,crit}$.
- Diagonal web cracking (force): $V \geq V_c$)
- Onset of stirrup yielding $\varepsilon_{st} = \varepsilon_{st,y}$
- Large inelastic strain in the stirrups (associated with the rate of strength loss with increasing ductility demand): $\varepsilon_{st} > \varepsilon_{st,y}$.

Shear Strength of Structural Members (Columns, Walls, Beams) at SD & NC

For columns, piers..

$$V_{shear} = V_c + V_N + V_s = k(\mu_\Delta) \cdot (0.16 \cdot \max(0.5; 100\rho_{tot}) \cdot \left(1 - 0.16 \min(5; \frac{L_s}{h}\right) \cdot \sqrt{f_c} \cdot 0.8A_g + \min\{N; 0.55A_c f_c\} \cdot \tan\alpha + A_{s,w} \cdot f_{yw} \cdot \left[\frac{d-d'}{s}\right]$$

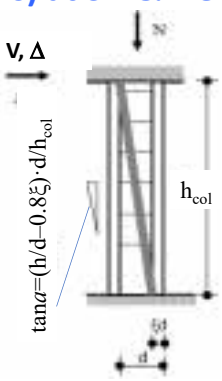

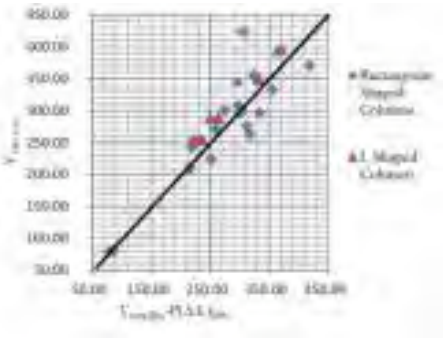

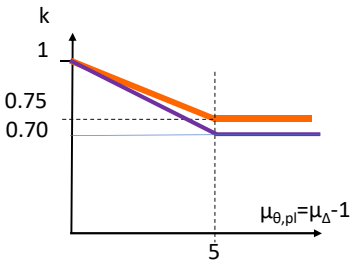

For walls

$$V_{sh} = k(\mu_\Delta) \cdot (0.85 \cdot (1 + 1.8 \cdot \min(0.15; \frac{N}{A_c f_c}) \cdot (1 - 0.2 \min(2; \frac{L_V}{h}) \cdot (1 + 0.25 \cdot max(1.75; 100\rho_{tot}) \cdot \sqrt{f_c} \cdot b_w \cdot z$$

Plastic Hinge Length: Inconsistencies of Empirical Expressions:

- Eurocode 8 – Part III, 2005 $L_{pl} = 0.1L_s + 0.17h + 0.24D_b f_y / f_c^{0.5}$
- **Priestley et. al. 1996** $L_{pl} = 0.08L_s + 0.022D_b f_y$
- **Classic Definition** $L_{pl} = (M_u - M_y) \cdot L_s / M_u + c$
- **Empirical Definition** $L_{pl} = 0.5d$

Alternative Definition of Plastic Hinge Length: $L_{pl} = (\varepsilon_o - \varepsilon_{sy}) \cdot \frac{E_{sh} \cdot D_b}{4 f_b^{res}}$

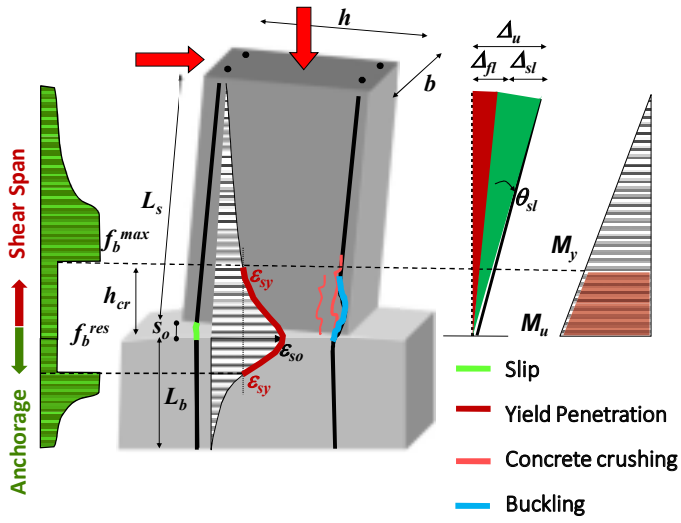

- The development of yielding flexural moment in plastic hinges of frame elements is synonymous with yielding strain penetration in shear span and anchorage.
- Yield penetration destroys interfacial bond between bar and concrete:

➔ Reduction of column plastic rotation due to flexure (reduction of strain development capacity of the reinforcement)

➔ Increase of bar pull-out contribution in the total column rotation.

Spread of inelasticity with increasing strain at the critical section:

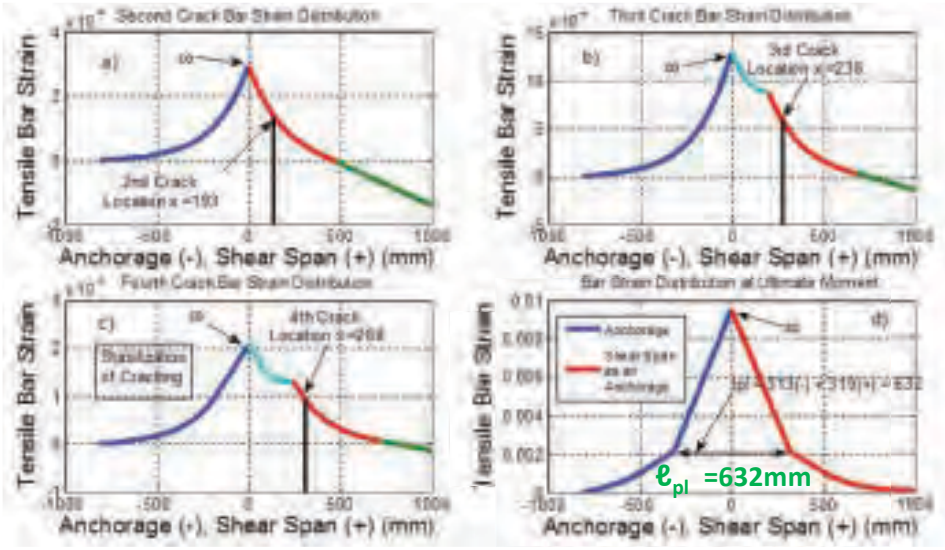

Plastic Hinge Length: Inconsistencies of Empirical Expressions:

- Eurocode 8 – Part III, 2005 $L_{pl} = 0.1L_s + 0.17h + 0.24D_b f_y / f_c^{0.5}$
- **Priestley et. al. 1996** $L_{pl} = 0.08L_s + 0.022D_b f_y$
- **Classic Definition** $L_{pl} = (M_u - M_y) \cdot L_s / M_u + c$
- **Empirical Definition** $L_{pl} = 0.5d$

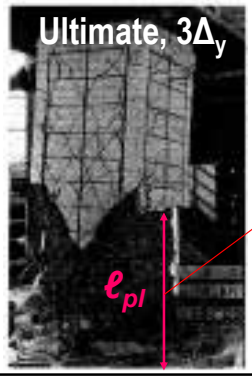

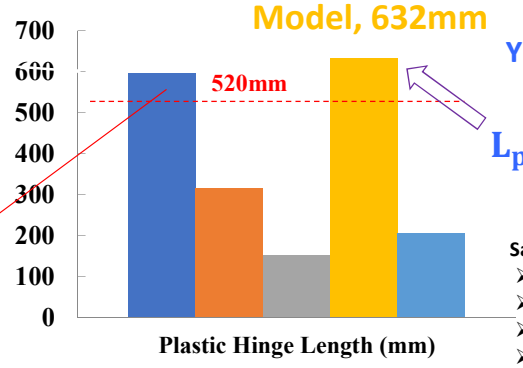

Yield Penetration Length:

$$L_{pl} = (\varepsilon_o - \varepsilon_{sy}) \cdot \frac{E_{sh} \cdot D_b}{4 f_b^{res}}$$

Saatcioglu and Ozcebe, 1989:

- Square column(350 mm)
- Shear span *Ls*=1000 mm
- Long. Reinf. 8Φ25, stirrups Φ10/75
- Concrete 34.8 MPa, Steel f_y=430MPa

Alternative Definition of Plastic Hinge Length in Walls Also:

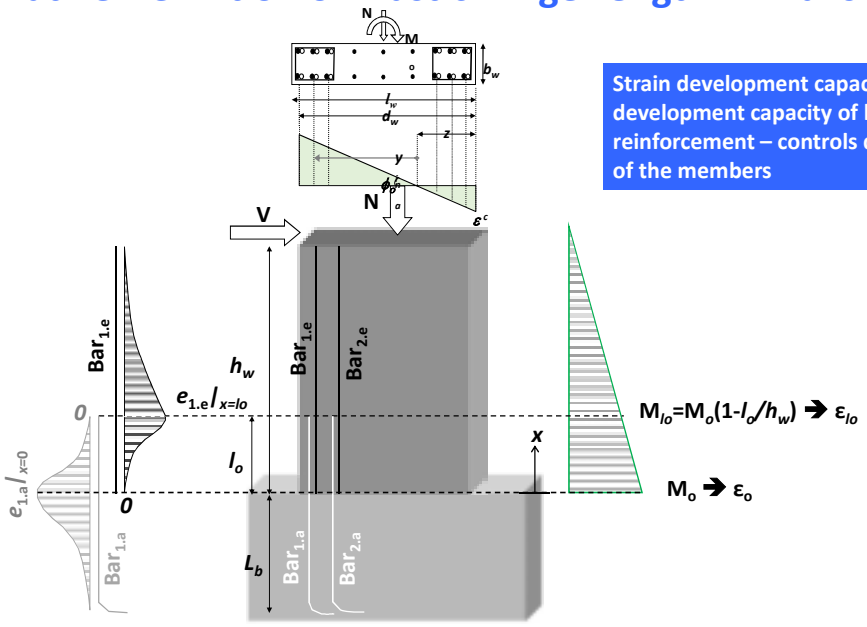

Strain development capacity, not stress development capacity of longitudinal reinforcement – controls deformability of the members

Damage Coefficients: r_K, r_R, r_{du}:

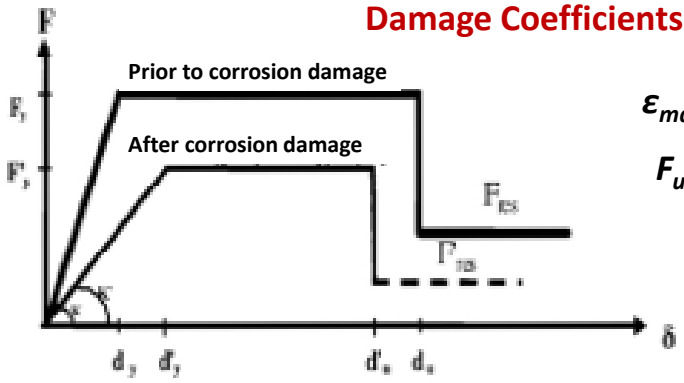

$$\varepsilon_{max(\%red)} = \varepsilon_{max} \cdot (1-4 \cdot x)$$

$$F_{u(\%red)} = F_u \cdot (1-1.15 \cdot x)$$

Low v_d: $\Delta_{u,cor} = \Delta_{u,o,1} \cdot (1-2.2 \cdot x)$

Moderate to High v_d: $\Delta_{u,cor} = \Delta_{u,o,2} \cdot (1-2.75 \cdot x)$

Low v_d: $V_{cor} = V_u \cdot (1-0.005 \cdot \theta \cdot x)$

Moderate to High v_d: $V_{cor} = V_u \cdot (1-0.008 \cdot \theta \cdot x)$

For θ = 0.5%:
$r_K = 1-0.0025 \cdot x$ $v_d < 0.2$
$r_K = 1-0.004 \cdot x$ $v_d > 0.2$

For θ = 2%:
$r_R = 1-0.01 \cdot x$ $v_d < 0.2$
$r_R = 1-0.016 \cdot x$ $v_d > 0.2$

For θ_{fail}:
$r_{du} = 1 - 2.2 \cdot x$ $v_d < 0.2$
$r_{du} = 1 - 2.75 \cdot x$ $v_d > 0.2$

Thank You

Session 3

Advanced Research in Earthquake Engineering

DEVELOPMENT OF TEST FACILITY AND CURRENT RESEARCH ON NON-STRUCTURAL COMPONENTS AND SYSTEMS AT NCREE

By Dr. J.-F. Chai, National Taiwan University of Science and Technology/ National Center for Research on Earthquake

Abstract

The test facilities developed for non-structural components and systems (NSCS) at NCREE will be introduced first. These facilities consist of a high frequency multi-axial simulation table (MAST) system, a rigid frame for dynamic tests of suspended large-area NSCS (e.g. ceiling system) and a double-slab frame for story-drift controlled NSCS (e.g. vertical piping system). Then, the current research topics on NSCS at NCREE will be introduced. One is the study of near-fault effect on the convective mode of storage liquid in tanks, which aims to estimate the slosh height and total volume of liquid splashing out of the tank due to the resonant effect of input velocity pulse. Another topic is the assessment for seismic performance of sprinkler piping systems. The numerical model of one typical sprinkler piping system was developed, and the seismic fragility curves were conducted for some specific failure modes using incremental demand analysis (IDA) method with the proposed evaluation criteria.

Keywords: test facilities for NSCS, MAST, convective mode, near-fault ground motions, sprinkler piping system, seismic fragility curve.

Biography

Dr. Juin-Fu Chai received his Ph.D. degree in 1995 from the Institute of Applied Mechanics in National Taiwan University. He is the Research Fellow and Division Head of NCREE, and is also a Professor in Department of Civil and Construction Engineering, National Taiwan University of Science and Technology. His research interests include seismic design, evaluation, qualification and retrofit for the non-structural components and systems, especially for the equipment in hospitals, nuclear power plants and Hi-Tech Fabs.

NARLabs
National Applied Research Laboratories

National Center for Research on Engineering Center

Development of Test Facility and Current Research on Non-structural Components and Systems at NCREE

Speaker: Dr. Juin-Fu Chai

Research Fellow and Division Head, NCREE
Professor, Dept. Civil and Construction Engineering, NTUST

NRC-MOST/NCREE Taiwan Workshop
October 7-9, 2019

NARLabs

OUTLINES

- Test Facility for NSCS at NCREE
- Current Research on NSCS at NCREE
  - Assessment for Seismic Performance of Piping Systems
  - Near-fault Effect on Convective Mode of Storage Liquid in Tanks

NARLabs

Test Facility for NSCS at NCREE

Test Facility for NSCS at NCREE

NCREE

4

Component

Material

Sub-system

System

Pretest with Scaled-down System

Acc. Controlled

Dis. Controlled

Full scale system

Rigid Frame for Suspended System

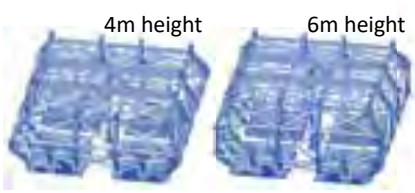

Double-Slab Framework (Dynamic)

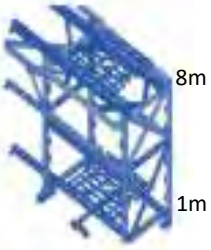

Multi-axial Simulation Table (MAST)

NCREE

5

- **Performance of MAST**
  - **Frequency: 0.5~50Hz**
  - **Industrial Standard**
    - ✓ **AC 156**
    - ✓ **GR-63-Core**
    - ✓ **IEEE 693 & IEEE 344**

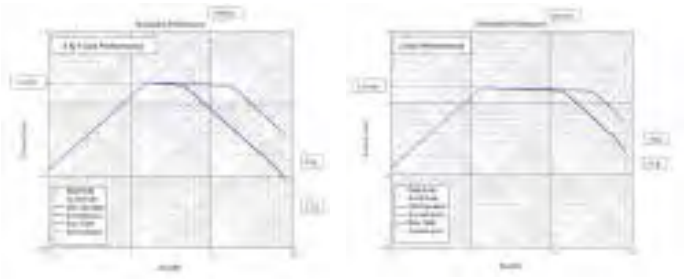

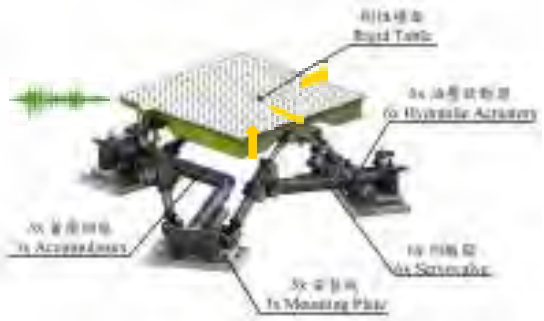

	X axis	Y axis	Z axis
stroke	±0.2 m	±0.2 m	±0.2 m
velocity	±2.0 m/s	±2.0 m/s	±1.65 m/s
Acceleration 3.5 ton 2.0 ton Bare Table	 ±5.5 g ±6.5 g ±20.0 g	 ±5.5 g ±6.5 g ±20.0 g	 ±14.0 g ±20.0 g ±30.0 g
Moment: 5.5 ton-m (Roll/ Pitch) 21 ton-m (Yaw)			

Rigid Frame for Suspended NSCS (1/3)

NCREE

6

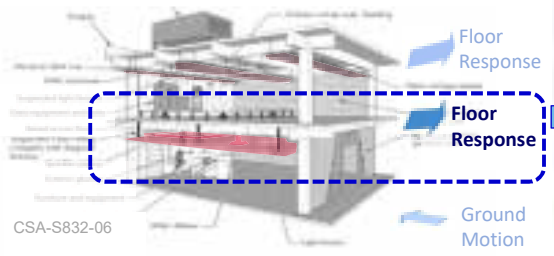

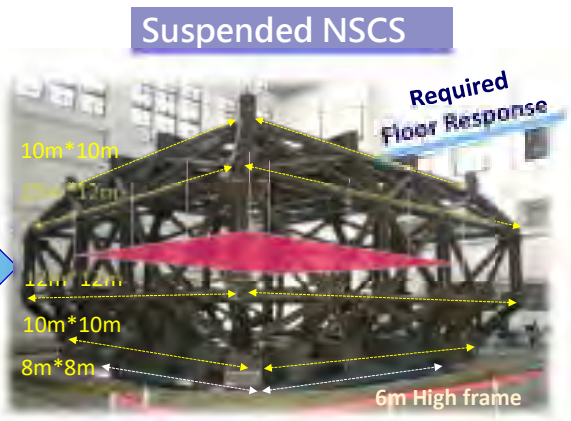

Rigid Frame for Suspended NSCS (2/3)

NCREE

7

- **Strategy for Amplification Effect**

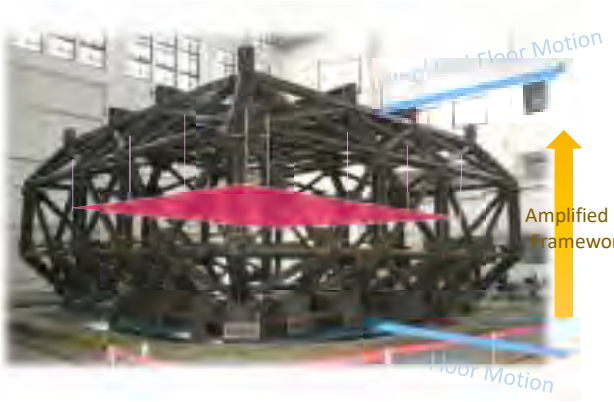

6m Framework (w/ central column)

Mode 1 (12.330Hz) Mode 2 (12.336Hz)

6m Framework (w/o central column)

Mode 1 (8.756 Hz) Mode 2 (12.375Hz)

Rigid Frame for Suspended NSCS (3/3)

NCREE

8

- **Strategy for Amplification Effect**
  - **AC156 RRS**

6m High Frame

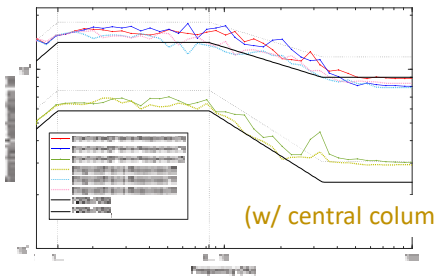

(w/ central column)

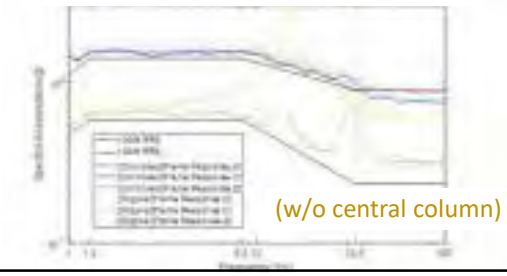

(w/o central column)

Double-Slab Frame

NCREE

9

- For story-drift control NSCS
  - Dynamic test

Adjustable Width

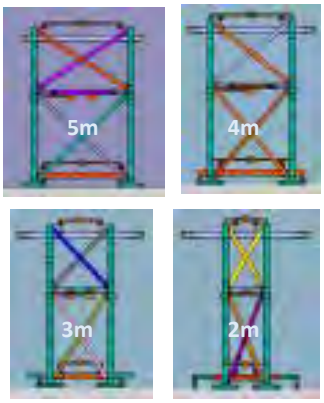

Double Sliding Floors with Linear Rails

Item	Specification
Force	Tension 200 kN ; Compression 400 kN
Stroke	±1000 mm (2000 mm totally)
Load Cell	±225 kN
Servo-valve	1000 gpm
Test Condition	0.5Hz sine wave 0.6g
	1Hz sine wave 1.5g
	2Hz sine wave 2g

High-Performance Actuators

NARLabs

Assessment for Seismic Performance of Piping Systems

Fire Protection Sprinkler Piping Systems

NCREE

- **Research Procedures for Sprinkler Piping Systems**

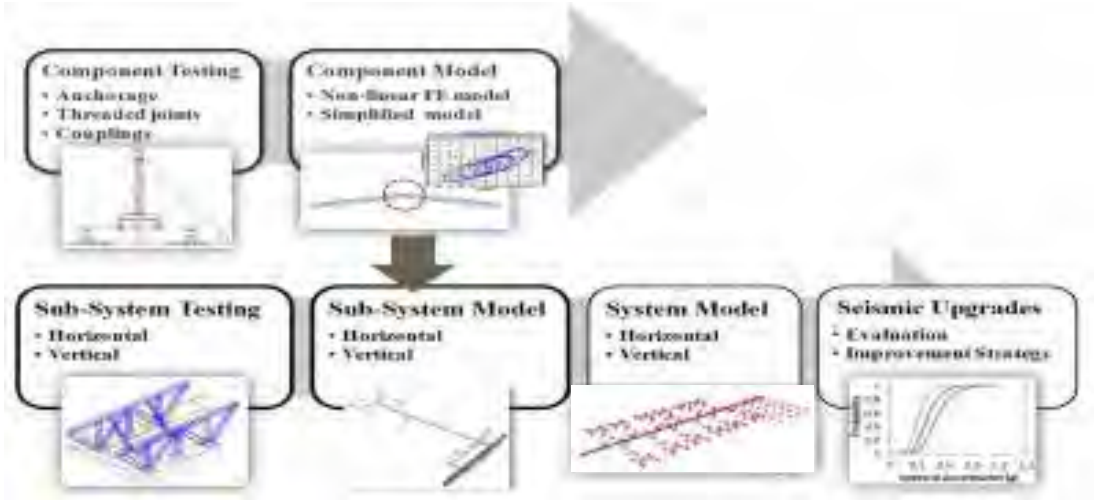

Component Testing

NCREE

- **Expansion Bolt**
  - ACI 355.2

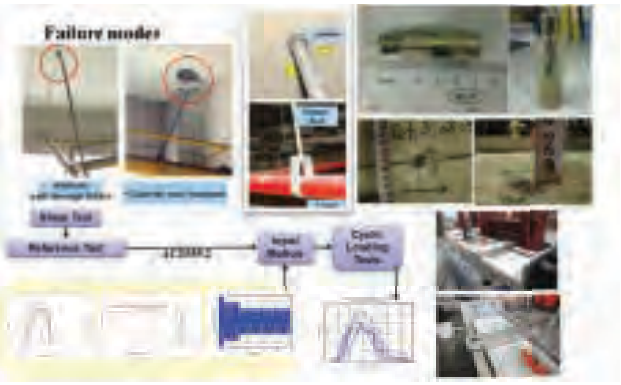

- **Piping Joint**
  - Threaded joint
  - Coupling joint

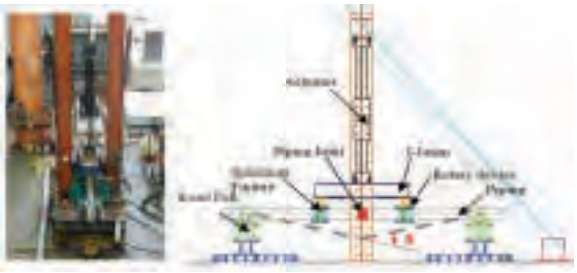

Shaking Table Test for Sub-system (1/2)

NCREE

- **Test Setup**

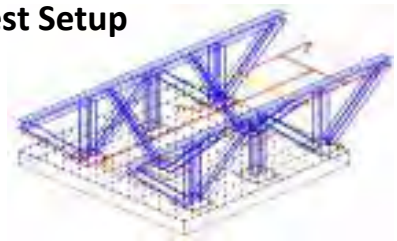

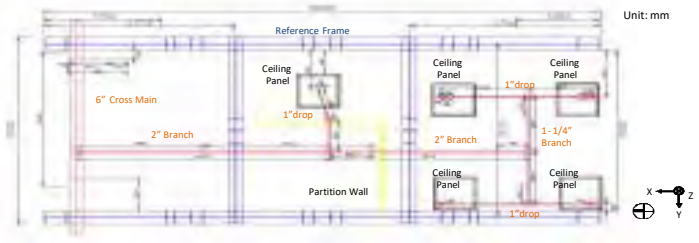

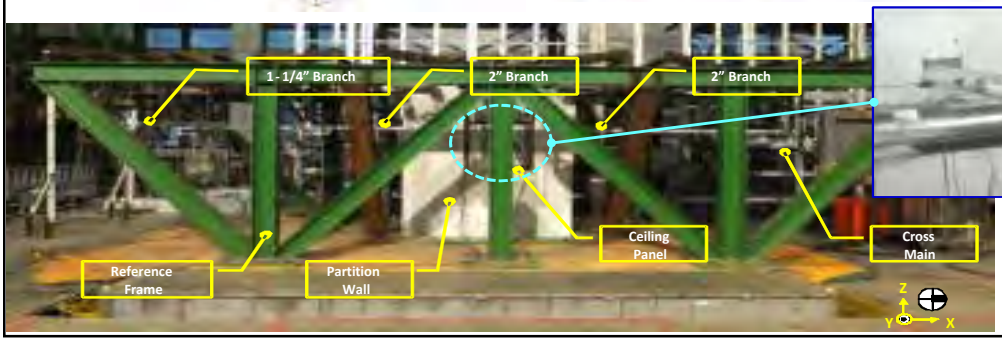

Shaking Table Test for Sub-system (2/2)

NCREE

- **Failure Mode**

Leakage on piping joint

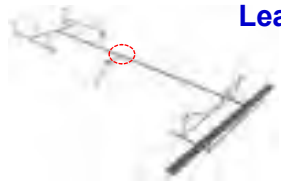

[redacted]

[redacted]

Original Configuration **(OC)**

Tearing of ceiling panel

[redacted]

w/ flexible hose **(FH)**

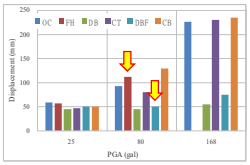

[redacted]

w/ double braces and flexible hose **(DBF)**